

Cotrimoxazole reduces systemic inflammation in HIV infection by modulating the gut microbiota and blunting immune cell activation

Authors: Claire D. Bourke^{1*#}, Ethan K. Gough^{2†#}, Godfrey Pimundu³, Annie Shonhai⁴, Chipo Berejena⁴, Louise Terry⁵, Lucas Baumard¹, Naheed Choudhry¹, Yusuf Karmali¹, Mutsa Bwakura-Dangarembizi⁴, Victor Musiime^{3,6}, Joseph Lutaakome⁷, Adeodata Kekitiinwa⁸, Kuda Mutasa⁹, Alexander J. Szubert¹⁰, Moira J. Spyer¹⁰, Jane R. Deayton^{1,5}, Magdalena Glass², Hyun Min Geum², Claire Pardieu¹, Diana M. Gibb¹⁰, Nigel Klein¹¹, Thaddeus J. Edens¹², A. Sarah Walker¹⁰, Ameer R. Manges^{2‡} and Andrew J. Prendergast^{1,9,10‡}

Affiliations:

¹Blizard Institute, Queen Mary University of London, London, UK

²School of Population and Public Health, University of British Columbia, Vancouver, Canada

³Joint Clinical Research Centre, Kampala, Uganda

⁴College of Health Sciences, University of Zimbabwe, Harare, Zimbabwe

⁵Royal London Hospital, Barts Health NHS Trust, London, UK

⁶Makerere University, College of Health Sciences, Department of Paediatrics and Child Health, Kampala, Uganda

⁷Uganda Virus Research Institute/MRC Uganda Research Unit on AIDS, Entebbe, Uganda

⁸Baylor – Uganda, Mulago Hospital, Kampala, Uganda

⁹Zvitambo Institute for Maternal and Child Health Research, Harare, Zimbabwe

¹⁰MRC Clinical Trials Unit at University College London, London, UK

¹¹UCL Great Ormond Street Institute of Child Health, London, UK

¹²Devil's Staircase Consulting, West Vancouver, British Columbia, Canada

Author Notes:

#These authors contributed equally to this work.

‡These authors contributed equally to this work.

†Current affiliations:

Ethan K. Gough: The Johns Hopkins Bloomberg School of Public Health, Baltimore, USA

Magdalena Glass: Canada's Michael Smith Genome Sciences Centre, Vancouver, Canada

*To whom correspondence should be addressed:

Claire D. Bourke, Centre for Genomics and Child Health, Blizard Institute, Barts and the
London School of Medicine and Dentistry, Queen Mary University of London, London,
U.K; c.bourke@qmul.ac.uk

One Sentence Summary: Long-term cotrimoxazole prophylaxis in HIV infection reduces systemic and intestinal inflammation by suppressing gut-resident Streptococci and modulating immune cell activation.

ABSTRACT

Long-term cotrimoxazole prophylaxis reduces mortality and morbidity in HIV infection but the mechanisms underlying these sustained clinical benefits are unclear. Here we investigate the impact of cotrimoxazole on systemic inflammation, an independent driver of HIV mortality. Using longitudinal plasma samples from HIV-positive Ugandan and Zimbabwean children receiving antiretroviral therapy in the ARROW trial, we show that inflammatory markers were lower after randomization to continue (n=144) versus stop (n=149) cotrimoxazole. This was not explained by clinical illness, HIV disease progression or nutritional status. Since sub-clinical enteropathogen carriage and HIV enteropathy can drive systemic inflammation, we explored the impact of cotrimoxazole on the microbiome and biomarkers of intestinal inflammation using fecal samples from ARROW. Although there were no global differences in microbiome community composition, viridans group Streptococci and streptococcal mevalonate pathway enzymes were lower among children randomized to continue (n=36) versus stop (n=36) cotrimoxazole. These changes were associated with lower levels of fecal myeloperoxidase, a biomarker of mucosal leukocyte activity. To isolate the direct effect of cotrimoxazole on immune activation from its effects on the microbiota, we established *in vitro* models of systemic and intestinal inflammation with and without cotrimoxazole treatment. Cotrimoxazole directly blunted pro-inflammatory cytokine production by blood leukocytes from HIV-positive (n=16) and HIV-negative (n=8) UK adults. It also reduced production of the neutrophil chemoattractant IL-8 by monolayers of inflamed gut epithelial cells. Together, these data demonstrate that cotrimoxazole prophylaxis reduces systemic and intestinal inflammation and that this is likely mediated both indirectly, through its antibiotic effects on the microbiota, and by direct

modulation of immune and epithelial cell activation. Synergy between these pathways may contribute to the sustained clinical benefits of long-term cotrimoxazole prophylaxis despite high antimicrobial resistance, providing a further rationale for extending coverage among people living with HIV in sub-Saharan Africa.

1

2 **INTRODUCTION**

3 In 2017, 36.9 million people were living with HIV globally and 940,000 died from AIDS-
4 related illnesses(1). To reduce mortality and morbidity(2, 3), World Health Organization
5 (WHO) guidelines recommend long-term cotrimoxazole prophylaxis for all people living
6 with HIV in areas with a high prevalence of malaria and/or severe bacterial infections,
7 regardless of HIV disease stage, CD4 cell count or use of antiretroviral therapy (ART)(4).
8 However, it is unclear why cotrimoxazole continues to effectively reduce mortality and
9 morbidity in the context of high rates of antimicrobial resistance and selection for resistant
10 pathogens with long-term use(2). There is therefore a need to better understand the effect of
11 cotrimoxazole on HIV pathogenesis.

12

13 Systemic inflammation is independently associated with mortality in HIV infection(5-7) and
14 this association is stronger in people living with HIV than among HIV-negative people(8).
15 Cotrimoxazole might plausibly confer benefits in HIV infection by reducing inflammatory
16 pathology, either indirectly by targeting pathogens that trigger inflammatory responses, or
17 directly by acting on cells that produce pro-inflammatory mediators. Animal models suggest
18 that other antibiotics confer anti-inflammatory benefits, including reduced monocyte
19 activation and cytokine production in SIV-infected minocycline-treated macaques(9), and
20 observational studies of HIV-positive adults in high-income settings suggest that
21 cotrimoxazole can reduce levels of plasma inflammatory biomarkers(10, 11). Data from
22 randomized trials and low-income settings are lacking and no studies have evaluated the
23 direct and indirect effects of cotrimoxazole on pro-inflammatory pathways in

25 people living with HIV.

26

27 HIV drives a chronic enteropathy, characterized by loss of villous architecture, increased
28 permeability, mucosal CD4+ T-cell depletion(12), leukocyte infiltration(13-15), and
29 microbial translocation(16-18), accompanied by increased pathogen carriage and an altered
30 microbiome(19-22); together, these changes contribute to systemic inflammation(16, 19, 23).

31 Cotrimoxazole prophylaxis could influence intestinal inflammation indirectly through
32 antibiotic effects on gut pathogens and/or the microbiome, or directly by affecting mucosal
33 leukocytes and gut epithelial cells(24, 25). Among HIV-positive Ugandan adults
34 cotrimoxazole was found to have limited effects on the gut microbiota(23), however the
35 effects of continuing cotrimoxazole on microbiota composition or HIV enteropathy have not
36 been assessed in a randomized trial or in children.

37

38 Cotrimoxazole comprises two folate pathway inhibitors, trimethoprim and sulfamethoxazole.
39 The hypothesis that cotrimoxazole can directly alter the pro-inflammatory responses of
40 circulating immune cells was first posited in 1970, following the observation that
41 intramuscular trimethoprim effectively prolonged skin graft retention in mice to the same
42 extent as the structurally similar immunosuppressive drug azathioprine(26). However,
43 subsequent *in vitro* studies of the direct effects of cotrimoxazole on innate and adaptive
44 immune cells have yielded conflicting results(27-32) and none have assessed its anti-
45 inflammatory effects on cells from HIV-positive individuals. Cotrimoxazole treatment of rats
46 also impacts absorption across the gut epithelium(24), suggesting that cotrimoxazole may

48 influence gut barrier function, a critical regulator of cross-talk between circulation and gut-
49 resident microorganisms.

50

51 Thus, cotrimoxazole prophylaxis confers long-term clinical benefits in HIV infection, which
52 are not entirely explained by its antibiotic effects(2, 3). Inconsistent evidence suggests that
53 cotrimoxazole may have anti-inflammatory properties, but conclusive data are lacking,
54 particularly among children living with HIV in low-income settings. We therefore capitalized
55 on a randomized trial of continuing versus stopping cotrimoxazole in HIV-positive children
56 in sub-Saharan Africa, to test the hypothesis that cotrimoxazole reduces systemic
57 inflammation. We then explored mechanistic pathways through which this may occur using a
58 combination of clinical data, stored specimens and *in vitro* models.

60 **RESULTS**

61 *Cotrimoxazole reduces systemic inflammation in HIV-positive children*

62 We have previously shown that randomization to continue compared to stopping
63 cotrimoxazole prophylaxis reduced hospitalization or death among HIV-positive children on
64 long-term ART in the ARROW trial in Uganda and Zimbabwe(33). Since inflammatory
65 biomarkers such as CRP and IL-6 are independently associated with mortality in HIV
66 infection, including in the ARROW cohort(5), we hypothesized that the benefits of
67 cotrimoxazole might be partly mediated through reductions in systemic inflammation.
68 Inflammatory biomarkers (CRP, IL-6, soluble (s)CD14 and TNF α) were quantified in
69 longitudinal cryopreserved plasma samples from children randomized to continue (n=144)
70 versus stop (n=149) cotrimoxazole within ARROW (**Fig. 1**).

71

72 Biomarkers were similar between groups at baseline (**Fig. 1A-D**), but subsequent CRP
73 concentrations from week-24 until the end of follow-up were lower in children randomized to
74 continue cotrimoxazole (**Fig. 1A**). IL-6 was also significantly lower among children
75 continuing cotrimoxazole, particularly at early time-points (**Fig. 1B**). There was no evidence
76 of global differences between groups in sCD14 (**Fig. 1C**) or TNF α (**Fig. 1D**). Plasma albumin
77 was significantly higher (median: 42 versus 41g/L, p=0.041) and total protein significantly
78 lower (76 versus 78g/L, p=0.038) in children continuing cotrimoxazole when measured at
79 week-48 (**Fig. 1E**), consistent with less systemic inflammation. Collectively these results
80 show definitively, through the randomized design, that cotrimoxazole reduces systemic
81 inflammation in HIV-positive children.

83 To estimate the clinical implications of these differences, we used our previously reported
84 relative risk estimates of adverse outcomes (defined as death, new or recurrent World Health
85 Organization clinical stage 4 events, or poor immunological response to ART) associated
86 with pre-ART pre-cotrimoxazole levels of CRP and IL-6 in ARROW(5). Stopping
87 cotrimoxazole in the current analysis led to increases in CRP and IL-6 levels at week-24 of
88 1.65-fold (stop 2.71mg/L versus continue 1.64mg/L; **Figure 1A**) and 1.18-fold (stop mean:
89 5.36pg/mL versus continue 4.54pg/mL; **Figure 1B**) respectively. Based on the previous
90 ARROW model for adverse outcomes this would correspond to an increased relative risk
91 among children stopping cotrimoxazole of 13% (95% CI: 4-24%) and 11% (95% CI: 4-18%)
92 within 24 weeks(5). Relative differences in CRP, which were maintained between
93 randomized groups throughout follow-up, peaked at week-48 (1.92-fold increase; 2.86mg/L
94 stop versus 1.49mg/L continue; **Figure 1A**), corresponding to an 18% (95% CI: 6-32%)
95 increased risk of adverse clinical outcomes. Thus, the cotrimoxazole-mediated differences
96 that we observed in CRP and IL-6 levels are clinically relevant to long-term survival, health
97 and immune restoration among children living with HIV.

98

99 ***Reduced systemic inflammation is not solely due to reduced clinical infections***

100 One explanation for reduced systemic inflammation among children continuing
101 cotrimoxazole prophylaxis would be an improved course of their HIV infection due to
102 reductions in intercurrent infections, particularly common but less severe infections not
103 leading to hospitalization or death(2, 33). However, there was no evidence of global
104 differences in the proportion of children with viral suppression (<80 HIV RNA copies/mL;

106 **Fig. 2A)** or in CD4+ T-cell percentages (%CD4; **Fig. 2B)** between randomized groups. There
 107 was also no evidence of differences between randomized groups in caregiver-reported cough
 108 (**Fig. 2C)**, fever (**Fig. 2D)**, nausea/vomiting (**Fig. 2E)** or abdominal pain (**Fig. 2F)** across the
 109 whole follow-up period or at individual time-points, with the exception of fever at week-12
 110 (7.4% continue versus 20.2% stop, $p=0.01$). Too few children had persistent, bloody or
 111 moderate-to-severe diarrhea, difficult/fast breathing and/or weight loss for comparison
 112 between groups. Thus, although the ARROW trial found that continuing cotrimoxazole
 113 reduced hospitalization or death(33), effects of cotrimoxazole on systemic inflammation were
 114 not explained by differences in HIV disease progression or symptomatic infections between
 115 groups.

116

117 *Cotrimoxazole prophylaxis does not affect nutritional status*

118 HIV-positive children frequently have malnutrition, and antibiotics (including cotrimoxazole)
 119 have been shown to improve growth(34) and slow weight-loss(35). We therefore compared
 120 anthropometry between randomized groups, reasoning that differences in systemic
 121 inflammation might be explained by underlying wasting or stunting(36, 37). We found no
 122 evidence of differences between groups in weight-for-age (**Fig. 2G)** or height-for-age Z-
 123 scores (**Fig. 2H)**, suggesting that lower inflammatory biomarkers were not driven by
 124 improved nutritional status in children continuing cotrimoxazole.

125

126 *Cotrimoxazole alters circulating CD4+ T-cell phenotype in HIV-positive children*

127 Although continuation of cotrimoxazole had no impact on total CD4 counts (**Fig. 2B)**, we

129 hypothesized that CD4+ T-cell phenotypes would differ between randomized groups.
130 Elevated systemic inflammation is frequently accompanied by T-cell activation in HIV
131 infection(38, 39) and we have previously shown that pre-ART pre-cotrimoxazole percentages
132 of proliferating (Ki67+) CD4+ T-cells are positively associated with systemic inflammation
133 in the ARROW cohort(5). T-cell immunophenotyping was conducted via flow cytometry in a
134 subset of Ugandan ARROW participants to determine the effects of cotrimoxazole on T-cell
135 activation and differentiation (stop n=48, continue n=47; **fig. S1A**). There was no evidence
136 for a difference between groups in the proportions of total CD4+ T-cells expressing the
137 activation marker HLA-DR or the proliferation marker Ki67 (**fig. S1B-C**). Children
138 continuing cotrimoxazole had higher percentages of recent thymic emigrant-like cells (RTE,
139 CD4+CD45RA+CD31+ T-cells; an indicator of thymic output(40)) than children stopping
140 prophylaxis (**fig. S1B**). There was no evidence of difference in proportions of naïve
141 (CD4+CD45RA+CD31-) and effector-memory (CD4+CD45RA-CD31-) T-cells or in the
142 expression of HLA-DR on any CD4+ T-cell sub-populations (**fig. S1C**). However, children
143 continuing cotrimoxazole had a lower percentage of proliferating (Ki67+) RTE and naïve T-
144 cells, particularly at later time-points post-randomization (**fig. S1D**); this did not correspond
145 to differences in mature or total CD4+ T-cells. Thus, cotrimoxazole prophylaxis is associated
146 with shifts in the composition and mobilization of the circulating T-cell pool, consistent with
147 reduced systemic inflammation(5).

148

149 ***Long-term cotrimoxazole suppresses fecal Streptococci but not Enterobacteriaceae***

150 Microbial consortia in the gut are disrupted by HIV infection, which contributes to local and
151 systemic inflammation(21, 41). Although we found no difference between randomized

153 groups in symptomatic intercurrent infections (**Fig. 2C-F**), we hypothesized that continuing
 154 cotrimoxazole would drive sustained sub-clinical differences in gut pathogens and
 155 commensals. We conducted whole metagenome shotgun sequencing of total fecal DNA from
 156 children randomized to continue (n=36 at week-84; n=33 at week-96) versus stop
 157 cotrimoxazole (n=36 at week-84; n=35 at week-96), compared bacterial community
 158 dissimilarity between randomized groups using the Bray–Curtis index and visualized this
 159 with non-metric multidimensional scaling (NMDS) plots (**Fig. 3A and B**). Hypothesis testing
 160 by permutation indicated no significant difference in community composition between
 161 children randomized to continue versus stop cotrimoxazole at either week-84 (**Fig. 3A**) or
 162 week-96 (**Fig. 3B**). However, zero-inflated beta regression analysis of microbiome
 163 characteristics identified seven bacterial species (*Alistipes onderdonkii*, *Eggerthella lenta*,
 164 *Clostridium bartlettii*, *Haemophilus parainfluenzae*, *Streptococcus mutans*, *Streptococcus*
 165 *parasanguinis* and *Streptococcus vestibularis*; **fig. S2**) and 11 protein families (Pfam; **fig.**
 166 **S3**), which mapped to *Streptococcus parasanguinis*, *Streptococcus salivarius* and
 167 *Haemophilus parainfluenzae*, that were consistently less abundant at both time-points in
 168 samples from children continuing versus stopping cotrimoxazole (relative abundance ratio
 169 <1) after FDR adjustment. The cotrimoxazole-affected Streptococcal species, all part of the
 170 Viridians group of Streptococci (VGS), largely fell in the quadrant of the NMDS ordination
 171 plot where the extremes of the treatment groups lay (**Fig. 3A and B**).

172

173 The relative abundance of Enterobacteriaceae, which includes common gastrointestinal
 174 pathogens (e.g. *Salmonella*, *Escherichia coli*, and *Shigella*) that are frequently resistant to
 175 cotrimoxazole(42-44), was not affected by cotrimoxazole at week-84 (relative abundance

177 ratio: 0.65, adjusted-p=0.108) and was increased in those continuing versus stopping
 178 cotrimoxazole at week-96 (4.48, adjusted-p<0.001).

179

180 To confirm the specific differences that we observed in VGS abundance according to
 181 cotrimoxazole we conducted high-resolution mapping of metagenome sequencing reads to
 182 Streptococci pangenome datasets using PanPhlAn software. PanPhlAn has a lower false
 183 positive rate for species-level identification and a better discrimination between samples
 184 containing the same versus different bacterial genomes than the MetaPhlAn software used for
 185 all bacterial species(45). Of the 140 fecal samples sequenced (both groups at week-84 and
 186 week-96), PanPhlAn identified 29 samples that were positive for the presence of any
 187 Streptococci (9 species were present: *S. salivarius*, *S. parasanguinis*, *S. mutans*, *S.*
 188 *vestibularis*, *S. australis*, *S. infantarius*, *S. oligofermentans*, *S. pasteurianus*, and *S. sanguinis*)
 189 and, of these, 20 samples that were positive for at least one of the 4 VGS species identified as
 190 being suppressed by cotrimoxazole using MetaPhlAn (7 at week-84 and 13 at week-96).
 191 Compared to MetaPhlAn, PanPhlAn identified a lower percentage of VGS-positive samples
 192 on account of its higher species-level resolution (**Fig. 3D** and **E**). Six samples from children
 193 continuing and 14 samples from children stopping cotrimoxazole were confirmed to be VGS-
 194 positive across both timepoints, corroborating VGS suppression by cotrimoxazole. Individual
 195 VGS species were confirmed to be present less often in children continuing cotrimoxazole
 196 (**Fig. 3E**); *S. salivarius* was found most frequently (6 continue samples versus 12 stop
 197 samples), followed by *S. vestibularis* (3 versus 10 samples), *S. parasanguinis* (1 versus 3
 198 samples) and *S. mutans* (0 versus 2 samples) across both timepoints; **Fig. 3E**.

199

201 Together, these findings show that continuing cotrimoxazole among HIV-positive children
202 treated with ART and cotrimoxazole for a median of 2 years prior to randomization does not
203 have additive effects on global microbiome community composition. However, continuation
204 of cotrimoxazole does drive specific alterations in fecal microbiome characteristics, with
205 suppression of VGS confirmed at species-level resolution but no evidence for sustained
206 increases on sub-clinical carriage of Enterobacteriaceae.

207

208 ***Cotrimoxazole suppresses the Streptococcal mevalonate pathway***

209 To understand the effect of cotrimoxazole on functional pathways within the differentially
210 abundant fecal microbiome species, we investigated microbial metabolic function by
211 quantifying the abundance of the full set of genes in a metabolic pathway regardless of the
212 taxa encoding them. Of the metabolic pathways, only mevalonate pathway I, which
213 influences neutrophil and monocyte recruitment and function(46, 47), was consistently
214 different according to cotrimoxazole treatment at both time-points. The abundance of
215 mevalonate pathway-associated genes was significantly lower in fecal samples from children
216 continuing cotrimoxazole (**Fig. 3C**). Of the enzyme-encoding genes within mevalonate
217 pathway I, those with identity to *Streptococcus parasanguinis* and *Streptococcus salivarius*
218 were significantly less abundant in the continue group (**Fig. 3C**).

219

220 Overall our fecal microbiome analyses identified a metagenomic signature of mevalonate
221 metabolism in VGS that is reduced with long-term cotrimoxazole prophylaxis (summarized
222 in **Fig. 3C**; analyses of all bacterial species and Pfam in **fig. S2** and **S3**, respectively).

224 ***Cotrimoxazole-induced changes in fecal Streptococci are associated with reduced intestinal***
 225 ***inflammation***

226 We next tested whether or not the cotrimoxazole-driven changes to microbiota composition
 227 and function influenced HIV enteropathy. We first compared levels of fecal inflammatory
 228 markers from a sub-set of Zimbabwean ARROW children with stored stool samples at week-
 229 84 and week-96 post-randomization to continue (n=37) or stop (n=38) cotrimoxazole. We
 230 chose myeloperoxidase, neopterin, alpha-1 antitrypsin and regenerating gene 1 β (REG1 β) as
 231 biomarkers of neutrophil and monocyte activity, macrophage and dendritic cell activation,
 232 gut permeability, and epithelial turnover, respectively(48). At week-84, fecal
 233 myeloperoxidase was significantly lower in children continuing versus stopping
 234 cotrimoxazole (median: 1694ng/mL versus 3178ng/mL, p=0.022; **Fig. 4A**), but there was no
 235 evidence of differences in neopterin, alpha-1-antitrypsin, or REG1 β between groups (p>0.15,
 236 **fig. S4A**). At week-96, fecal myeloperoxidase tended to be lower in children continuing
 237 cotrimoxazole (1262 versus 1473ng/mL, p=0.093; **Fig. 4B**), but there was no evidence of
 238 differences in neopterin, alpha-1-antitrypsin or REG1 β between groups (p>0.15, **fig. S4B**).
 239 Since myeloperoxidase is an abundant peroxidase enzyme in monocytes and neutrophils that
 240 perpetuates granulocyte activation(49) and both monocytes and neutrophils home to the gut
 241 mucosa during HIV infection(14, 15), these observations suggest that cotrimoxazole reduces
 242 innate immune cell activity in the gut.

243

244 Of the bacterial species suppressed by cotrimoxazole, *Streptococcus mutans*, *Streptococcus*
 245 *vestibularis*, *Streptococcus parasanguinis*, and *Haemophilus parainfluenzae* were positively
 246 associated with myeloperoxidase levels at week-96 (*Streptococcus* spp. summarized in **Fig.**

248 **4C**; analysis of all cotrimoxazole-affected species is shown in **fig. S5**), after adjustment for
 249 age, sex, and cotrimoxazole group. Myeloperoxidase levels were also positively associated
 250 with Pfam that were differentially abundant according to cotrimoxazole treatment, 5 with
 251 identity to *Streptococcus parasanguinis*, 2 to *Streptococcus salivarius*, 2 to *Haemophilus*
 252 *parainfluenzae*, and 1 to *Eubacterium bioforme* at week-96 (Pfam with identify to
 253 *Streptococcus* spp. summarized in **Fig. 4C**; analysis of all cotrimoxazole-affected Pfam is
 254 shown in **fig. S6**). Overall mevalonate pathway I abundance was significantly associated with
 255 higher myeloperoxidase at week-96 and tended towards a positive association at week-84
 256 (**Fig. 4C**). Of the mevalonate pathway I enzymes that differed between randomized groups,
 257 only those with identity to *Streptococcus parasanguinis* and *Streptococcus salivarius* had a
 258 significant positive association with myeloperoxidase (**Fig. 4C**).

259

260 We therefore show that all VGS components suppressed by cotrimoxazole (**Fig. 3C**) were
 261 also significantly positively associated with myeloperoxidase at week-96 (**Fig. 4C**),
 262 suggesting that sub-clinical effects of cotrimoxazole on VGS abundance and function
 263 contribute to lower intestinal inflammation among children continuing cotrimoxazole.

264

265 *Cotrimoxazole blunts pro-inflammatory cytokine responses in vitro*

266 Having established that continuation of cotrimoxazole reduces both systemic and intestinal
 267 inflammation among HIV-positive children on ART, we next investigated whether
 268 cotrimoxazole has direct immunomodulatory properties. In order to isolate any direct effects
 269 of cotrimoxazole on immune cells from its impact on the microbiota, we optimized an *in vitro*

271 model of whole blood cytokine responses to bacterial and fungal antigens: heat-killed
272 *Salmonella typhimurium* (HKST), which activates immune cells via Toll-like receptor (TLR)
273 2, 4 and 5; purified *Escherichia coli* lipopolysaccharide (LPS), which engages TLR4; and the
274 *Saccharomyces cerevisiae* cell-wall component zymosan, which engages TLR2 and dectin-1.
275 Antigens that engage innate pathogen recognition receptors were chosen for these assays to
276 reflect the elevated microbial translocation reported during HIV infection, which drives
277 systemic inflammation and immune activation(7, 16, 19, 41). Cotrimoxazole dose was chosen
278 to reflect maximum (high-dose; 8µg/mL trimethoprim and 200µg/mL sulfamethoxazole) and
279 minimum (low-dose; 2µg/mL trimethoprim and 50µg/mL sulfamethoxazole) serum
280 concentrations in HIV-positive patients taking cotrimoxazole(50). Laboratory cotrimoxazole
281 preparations were confirmed to have antibiotic activity (**fig S7A**) and had no impact on cell
282 viability at the concentrations used for subsequent experiments (**fig. S7B-D**).

283

284 Since systemic inflammation can affect subsequent immune cell responses to stimuli, we
285 predicted that the *in vitro* effects of cotrimoxazole might be influenced by the pre-existing
286 inflammatory milieu. We therefore obtained blood samples from cotrimoxazole-untreated
287 HIV-positive (ART-treated (n=6) and ART-naïve (n=10)) and HIV-negative UK adults (n=8,
288 **table S1**) with confirmed differences in baseline systemic inflammation, circulating
289 monocytes, and T- cell activation (**fig. S8**). There was no difference between the groups in
290 spontaneous cytokine production in unstimulated cultures over 24h (**Fig. 5**).

291

292 Treatment with high-dose cotrimoxazole significantly reduced levels of HKST-, LPS- and

294 zymosan-induced TNF α (**Fig 5A**) and IL-6 (**Fig 5B**) relative to control treatment with drug
295 diluent alone (DMSO) in one or more group. This was particularly evident for HKST- and
296 LPS-induced TNF α and LPS- and zymosan-induced IL-6, which were significantly lower
297 across all three clinical groups. LPS- and zymosan-induced TNF α and zymosan-induced IL-6
298 were also significantly reduced by low-dose cotrimoxazole in the HIV-positive ART-naïve
299 group (**Fig 5A and B**).

300

301 These observations confirm our hypothesis that cotrimoxazole directly modulates pro-
302 inflammatory immune cell activation by pathogen antigens, both in HIV-positive and in HIV-
303 negative individuals independently of the effect of oral cotrimoxazole prophylaxis on
304 microbiome composition or intestinal inflammation.

305

306 *Cotrimoxazole affects monocyte but not T-cell cytokine production*

307 To determine the immune cell types modulated by cotrimoxazole, we evaluated intracellular
308 TNF α production and surface expression of HLA-DR by monocytes and T-cells during 6h
309 PBMC culture with or without high-dose cotrimoxazole. Cotrimoxazole reduced the
310 proportion of TNF α ⁺ monocytes after HKST stimulation relative to control-treated cultures
311 in the HIV-negative group but not in the HIV-positive groups (**Fig. 5C**). Cotrimoxazole did
312 not alter HKST-induced up-regulation of HLA-DR by monocytes (**Fig. 5C**). Cotrimoxazole
313 also had no effect on the proportion of TNF α ⁺ or HLA-DR⁺ CD4⁺ or CD8⁺ T-cells after
314 polyclonal stimulation with staphylococcal enterotoxin B (SEB; **Fig. 5D and E**). Thus,
315 although cotrimoxazole reduces pro-inflammatory cytokine production by blood leukocytes

317 and TNF α production by monocytes specifically, it does not directly reduce monocyte
318 maturation or T-cell activation as assessed by HLA-DR expression.

319

320 ***Cotrimoxazole reduces IL-8 production by gut epithelial cells***

321 The gut epithelium provides a barrier between the microbiota and gut mucosal immune cells,
322 responds to TLR ligands, and produces leukocyte chemoattractants under inflammatory
323 conditions; direct effects of cotrimoxazole on epithelial cell function could contribute to its
324 anti-inflammatory effects. To isolate direct effects of cotrimoxazole on the epithelial barrier
325 from its impact on the microbiota, we used transwell cultures of the Caco-2 human colonic
326 epithelial cell-line as a well-established model of gut epithelium. We induced epithelial
327 inflammation with IL-1 β and evaluated the effect of cotrimoxazole on four epithelial
328 functions that could influence cross-talk between microbes and mucosal immune cells:
329 epithelial integrity (trans-epithelial resistance, TEER), epithelial cell death (%Lactose
330 dehydrogenase (LDH) activity), apical-to-basal translocation of a fluorescent dye (%Lucifer
331 Yellow passage, a proxy for microbial translocation), and production of the neutrophil
332 chemoattractant IL-8 (**Fig. 6A**). We used higher cotrimoxazole concentrations for these
333 experiments than for whole blood cultures to reflect the higher concentrations found in the
334 gut lumen following oral dosing, after first titrating cotrimoxazole in Caco-2 cultures to
335 identify a dose that did not differ in cytotoxicity from DMSO controls (1mg/mL; **Fig. 6B**).

336

337 Cotrimoxazole treatment throughout Caco-2 growth did not significantly alter the rate of
338 monolayer confluence (mean TEER/plate >800 Ω ; **Fig. 6C**), Δ TEER, %LDH activity or

340 %Lucifer yellow passage under inflammatory conditions relative to DMSO control-treatment
341 (1, 10 or 100 μ g/mL IL-1 β for 24h; **Fig. 6D**). However, cotrimoxazole-treated monolayers
342 produced significantly less IL-8 than control-treated cultures when the inflammatory stimulus
343 was highest (100 μ g/mL IL-1 β , p=0.003) and tended to produce less IL-8 at lower IL-1 β
344 concentrations than DMSO-treated cultures (1 μ g/mL, p=0.257, and 10 μ g/mL, p=0.095; **Fig.**
345 **6D**).

346

347 Taken together, these experiments suggest that cotrimoxazole can directly modulate IL-8
348 production by gut epithelial cells independently of its effects on the microbiome, which may
349 contribute to reduced neutrophil recruitment to the intestinal mucosa under inflammatory
350 conditions.

352 **DISCUSSION**

353 Inflammation drives morbidity and mortality among people living with HIV. There is
354 therefore growing interest in identifying adjunctive anti-inflammatory agents to improve
355 clinical outcomes with ART(51-54). Cotrimoxazole is currently recommended long-term for
356 children and adults living with HIV in settings with high prevalence of malaria or invasive
357 bacterial infections, although global coverage remains poor(4, 55). We show here that long-
358 term continuation of cotrimoxazole prophylaxis reduces systemic inflammation in ART-
359 treated children living with HIV in sub-Saharan Africa and demonstrate several novel
360 mechanisms through which this may occur, including antibiotic effects on the fecal
361 microbiome and direct anti-inflammatory effects on leukocyte and gut epithelial cell cytokine
362 production *in vitro*. Synergy between antibiotic and anti-inflammatory pathways may explain
363 the sustained clinical benefits of cotrimoxazole for people living with HIV in settings where
364 the prevalence of cotrimoxazole-resistant pathogens is high(3, 33) and provides an additional
365 rationale for improving coverage of cotrimoxazole prophylaxis in sub-Saharan Africa.

366

367 We first exploited available samples from the ARROW trial, allowing us to show
368 definitively, using the randomized stop-versus-continue design, that the systemic
369 inflammatory biomarkers CRP and IL-6 are reduced by cotrimoxazole. We also observed
370 cotrimoxazole-mediated changes in serum proteins and circulating naive CD4+ T-cell
371 mobilization consistent with reduced systemic inflammation. Whilst it would be desirable in
372 future studies to include more comprehensive infection screening, we found no evidence for
373 differences in caregiver-reported symptoms of intercurrent illnesses between the

375 randomized groups. We therefore reasoned that the long-term benefits of continuing
376 cotrimoxazole may be partially mediated through its anti-inflammatory effects. Previous
377 studies have demonstrated that, even with very early initiation of ART, not all circulating
378 inflammatory mediators are normalized when HIV viremia is controlled(56, 57) and high
379 levels of certain inflammatory mediators continue to predict morbidity and mortality(5-7, 58).
380 We have previously shown that pre-ART pre-cotrimoxazole levels of both CRP and IL-6, but
381 not TNF α or sCD14, predicted the relative risk of three important clinical outcomes
382 (mortality, WHO stage 4 clinical events and poor CD4 reconstitution) in the ARROW trial; a
383 2-fold increase in baseline CRP or IL-6 was independently associated with 19% and 54%,
384 increased risk of these outcomes, respectively(5). Absolute mortality rates are lower among
385 HIV-positive children after initiating ART and cotrimoxazole; however, based on our
386 predictions from pre-ART biomarker levels, the reductions in CRP and IL-6 that we
387 demonstrate among children continuing cotrimoxazole in the current study would reduce
388 their relative risk of adverse outcomes over the subsequent 24 weeks post-randomization by
389 13% and 11%, respectively compared to children who stopped cotrimoxazole. These
390 estimates highlight that the anti-inflammatory benefits of cotrimoxazole are clinically
391 meaningful, and may have substantial impact at a population level, given the ultimate goal of
392 universal coverage of cotrimoxazole among people living with HIV.

393

394 Soluble inflammatory mediators appear to be better predictors of poor clinical outcomes than
395 T-cell activation among people living with HIV in resource-limited settings(8). In a subgroup
396 of children in Uganda, we were able to evaluate the impact of cotrimoxazole on T-cell
397 immunophenotype. We observed lower percentages of proliferating naïve CD4+ T- cells

399 among children continuing cotrimoxazole, which we interpret as a beneficial phenotype since
 400 elevated CD4+ T-cell proliferation without a corresponding increase in total counts is
 401 associated with depletion of the naïve T-cell pool(59). Unfortunately, ARROW sample
 402 limitations meant that our analysis of circulating immune cell activation was limited to HLA-
 403 DR expression on CD4+ T-cells, for which we did not identify an effect of continuing
 404 cotrimoxazole. To more comprehensively assess the effects of *in vivo* cotrimoxazole on
 405 immune cells, future studies should include a wider range of T-cell surface activation markers
 406 and assessment of CD8+ T-cell and innate immune cell activation.

407

408 We went on to explore the underlying factors driving the cotrimoxazole-mediated differences
 409 in circulating CRP and IL-6. Systemic inflammation in HIV infection is partly driven by
 410 enteropathogen carriage and chronic enteropathy(12-14, 16) and the effect of cotrimoxazole
 411 on these domains has not been previously characterized. Using fecal samples from a sub-set
 412 of children randomized within ARROW, we demonstrated that VGS were less abundant in
 413 children continuing prophylaxis at both week-84 and week-96 post-randomization. Since
 414 speciation of VGS can be challenging, we confirmed the species-level differences that we
 415 observed according to cotrimoxazole using high-resolution mapping of metagenome
 416 sequencing reads to Streptococcal pangenomes databases(45). These analyses confirmed that
 417 *S. salivarius*, *S. vestibularis*, *S. parasanguinis* and *S. mutans* were specifically suppressed by
 418 cotrimoxazole. The effects of cotrimoxazole on VGS are particularly striking since global
 419 microbiome community composition did not significantly differ between randomized groups,
 420 likely because these children had been receiving cotrimoxazole with ART for a median of 2
 421 years prior to randomization(33). VGS are a heterogeneous group of bacteria, which can

423 be both commensal and pathogenic(60); they are frequently observed in the oral microbiome,
 424 but are found throughout the healthy human gut(61, 62). VGS are also enriched in fecal
 425 samples from children with stunting(63), a form of chronic malnutrition associated with
 426 elevated systemic inflammation(64), suggesting that so-called ‘decompartmentalization’ of
 427 microbial communities along the gastrointestinal tract and immune activation may be
 428 interrelated. For example, VGS express a range of immune-stimulatory antigens, and potently
 429 activate innate immune cell cytokine production *in vitro*(65). In contrast to changes in VGS,
 430 we found no evidence for suppression of Enterobacteriaceae, a taxonomic group including
 431 pathogens causing severe bacterial infections among people living with HIV, which are
 432 frequently resistant to cotrimoxazole in sub-Saharan Africa(42-44). Thus, whilst sub-clinical
 433 carriage of Enterobacteriaceae might be expected to drive systemic inflammation, this did not
 434 appear to be the case in this cohort. Our microbiome analyses focused on later time-points
 435 post-randomization, due to sample availability; there may therefore have been additional
 436 antibiotic effects of cotrimoxazole at earlier time-points and other anatomical sites, which we
 437 were not able to investigate.

438

439 We went on to explore the relationship between cotrimoxazole-mediated changes in the
 440 microbiota and biomarkers of intestinal inflammation. Children randomized to continue
 441 cotrimoxazole had lower levels of fecal myeloperoxidase, an antimicrobial peroxidase
 442 enzyme abundantly expressed in neutrophil granules and a biomarker of enteropathy, which
 443 was associated with a number of microbiota characteristics. Of the cotrimoxazole-affected
 444 VGS, *Streptococcus mutans*, *Streptococcus parasanguinis* and *Streptococcus vestibularis*
 445 were positively associated with fecal myeloperoxidase levels. Myeloperoxidase more readily

447 kills group A and group B streptococci than VGS *in vitro*(66). Thus, VGS may have a
 448 selective advantage over more myeloperoxidase-susceptible species in HIV enteropathy,
 449 during which myeloperoxidase-producing innate leukocytes accumulate in the gut(15, 67).
 450 Our data indicate that these novel sub-clinical antibiotic effects of cotrimoxazole on VGS
 451 contribute to reduced intestinal inflammation. A recent study of experimentally induced
 452 suppression of gram-positive bacteria in rhesus macaques with vancomycin prior to SIV
 453 infection, indicated that antibiotic-induced dysbiosis was not associated with differences in
 454 IL-6 or CD4+ T cell activation in the mesenteric lymph nodes relative to SIV infection
 455 alone(68). Thus, the timing of antibiotic treatment (before SIV infection in macaques and
 456 after HIV infection in humans), existing microbiota composition, history of ART treatment,
 457 intercurrent infection prevalence and antibiotic specificity all likely influence the relationship
 458 between antibiotic-induced changes in the microbiota and intestinal inflammation.

459

460 Our microbiome analyses highlighted bacterial gene markers of mevalonate pathway I,
 461 predominantly mapping to VGS, which decreased with cotrimoxazole continuation and were
 462 positively associated with fecal myeloperoxidase. The mevalonate pathway is one of two
 463 metabolic processes that produce isoprenoids, a diverse class of naturally occurring organic
 464 precursors in eukaryote cholesterol synthesis and prokaryote cell wall peptidoglycan (a TLR2
 465 ligand)(69). Several *in vitro* studies indicate that inhibition of mevalonate pathway
 466 components impairs innate leukocyte recruitment and function, providing a precedent for
 467 how inhibition of VGS mevalonate metabolism by cotrimoxazole might influence HIV
 468 enteropathy. For example, inhibiting farnesyl pyrophosphate synthesis reduces neutrophil
 469 priming by IL-8(70), and inhibiting hydroxymethylglutaryl-CoA reductase (HMG-CoA)

471 activity reduces IL-6 and IL-8 production by monocytes(71) and trans-epithelial migration by
472 neutrophils(51, 54). HMG-CoA with identity to *Streptococcus parasanguinis* and
473 *Streptococcus salivarius* was among the mevalonate pathway enzymes that we found to be
474 less abundant in children continuing cotrimoxazole. Given these observations, our data
475 suggest that cotrimoxazole prophylaxis in HIV-positive children may reduce innate leukocyte
476 recruitment and activation in the gut indirectly by suppressing VGS and their
477 myeloperoxidase-promoting mevalonate pathway.

478

479 Leukocytes are an abundant source of pro-inflammatory cytokines, which are synthesized and
480 released following ligation of innate pathogen recognition receptors including TLRs.

481 Multiple studies have demonstrated higher levels of circulating microbial products that could

482 trigger these pathways during HIV infection, including the TLR4 ligand LPS(11, 16). We

483 developed an *in vitro* model of leukocyte activation by TLR ligands to isolate direct anti-

484 inflammatory effects of cotrimoxazole from its antibiotic effects on pathogenic and

485 commensal microbes, using blood samples from HIV-negative and HIV-positive UK adults

486 who were not receiving cotrimoxazole. Physiologically relevant cotrimoxazole doses had a

487 consistent inhibitory effect on *in vitro* whole blood TNF α and IL-6 production elicited via

488 TLR2, 4 and 5 signaling, suggesting that modulation of innate pro-inflammatory cytokine

489 production is a property of cotrimoxazole *per se*, and occurs independently of its antibiotic

490 properties, pre-existing inflammation or ART exposure. Intracellular cytokine staining of

491 PBMC suggested that monocyte rather than T-cell cytokine production was most affected by

492 cotrimoxazole, albeit less consistently than the effect seen on whole blood cytokine

493 responses. Our demonstration of direct modulation of pro-inflammatory cytokine production

495 by blood leukocytes clarifies a longstanding theory that cotrimoxazole modulates immune
 496 responses in mice via an undefined mode-of-action(26), for which subsequent studies have
 497 yielded opposing conclusions using *in vitro* models of innate(27-29, 31, 32) and adaptive(28,
 498 30, 31) immune cell function. Most existing studies were conducted several decades ago and
 499 used inconsistent immunoassays; our study has the advantage of more recent functional
 500 immunology assays and was informed by the ARROW trial findings, which highlighted pro-
 501 inflammatory cytokine production as a clinically relevant pathway(5). The *in vitro* effects
 502 observed were quantitatively subtle; however, our prior analysis of pre-ART IL-6 levels in
 503 plasma from ARROW suggest that small differences are independently associated with
 504 reduced relative risk of adverse clinical outcomes among HIV-positive children(5).
 505 Additional studies are necessary to characterize the pharmacology of cotrimoxazole-mediated
 506 immunosuppression, the nature of its interaction with TLR signaling and evaluate its
 507 potential therapeutic value in other inflammatory disorders. Our observations in UK adults
 508 provide a rationale for further exploration of the effects of cotrimoxazole on innate and
 509 adaptive immune cell function in HIV-positive and HIV-negative children.

510

511 Using a separate *in vitro* model we found that long-term cotrimoxazole treatment also
 512 reduced production of the neutrophil chemoattractant IL-8 by inflamed epithelial cells. This
 513 is a novel putative pathway through which cotrimoxazole could directly contribute to reduced
 514 neutrophil recruitment and myeloperoxidase production in the gut mucosa during HIV
 515 enteropathy. Cotrimoxazole did not alter epithelial characteristics associated with barrier
 516 function (epithelial integrity, dye translocation or cell viability) *in vitro*. However, it remains
 517 possible that these pathways are altered *in vivo* through drug effects on components of the

519 gut barrier, such as the mucus layer(24) and expression of tight junction proteins(68), which
520 we did not model. Biopsy specimens were not available from children in ARROW; however,
521 evaluation of the effect of cotrimoxazole on gut biopsies from HIV-positive donors and *in*
522 *vitro* using 3-dimensional gut models, which more accurately mimic trans-epithelial
523 transport, would be desirable for extending this work. Since VGS express abundant TLR2
524 ligands and the Caco-2 line express low levels of TLR2(72), alternative epithelial cell lines or
525 primary epithelial cells with intact TLR2 signaling would be required to explore the
526 relevance of cotrimoxazole-mediated changes to VGS metabolism to epithelial barrier
527 function *in vitro*.

528

529 Collectively, this study identifies cotrimoxazole as an immunomodulator as well as an
530 antibiotic, which reduces both systemic and intestinal inflammation in HIV infection. We
531 have identified an anti-inflammatory agent that has the advantage of being routinely
532 recommended with ART in sub-Saharan Africa, widely available, well-tolerated and low-
533 cost(2). Our study raises the possibility that antibiotics other than cotrimoxazole may confer
534 anti-inflammatory benefits that contribute to their impact at scale in low-income settings, for
535 example the recent demonstration of reduced child mortality following mass administration
536 of azithromycin(73). The potential for antibiotics to have accessory benefits to direct
537 pathogen killing, contributes to current debate around antibiotic stewardship in settings where
538 antimicrobial resistance is already high and particularly for conditions such as HIV, where
539 chronic inflammation combines with intercurrent infection to exacerbate clinical outcomes.
540 Whether or not cotrimoxazole has clinical benefits for people living with HIV in high-income
541 countries, where long-term prophylaxis is not currently recommended, warrants further study

543 since ART alone does not fully prevent pathology. The demonstration of its anti-
544 inflammatory benefits in this study should drive renewed efforts for universal cotrimoxazole
545 coverage to improve clinical outcomes for all people living with HIV in sub-Saharan Africa.

547 **MATERIALS & METHODS**

548 ***Ethical approval***

549 The Antiretroviral Research for Watoto trial (ARROW; ISRCTN Registry#
550 ISRCTN24791884; <http://www.isrctn.com/ISRCTN24791884>) and use of biological
551 specimens collected from children enrolled in ARROW were approved by Research Ethics
552 Committees in Uganda, Zimbabwe, and the UK. Written informed consent from all
553 caregivers and assent from participants, where appropriate, was obtained as previously
554 described(33, 74).

555

556 Approval to assess the effect of *in vitro* cotrimoxazole on immune cell activation in adult
557 volunteers with and without HIV infection was provided by the UK National Health Service
558 Research Authority (NHS IRAS project ID: 209553; Research Ethics Council reference:
559 17/WM/0018) and the Research Ethics Committee of Queen Mary University of London. All
560 participants provided written informed consent.

561

562 ***ARROW randomized trial***

563 Cryopreserved plasma and fecal samples were obtained from children enrolled in ARROW,
564 an open-label, randomized, parallel-group trial among HIV-positive children. One
565 randomization within ARROW recruited children and adolescents (median age: 7.9 years,
566 interquartile range (IQR): 4.6, 11.1) who had been receiving ART for >96 weeks in the trial
567 (median duration of ART: 2.1 years, IQR: 1.8, 2.2) at medical centers in Uganda (Joint
568 Clinical Research Centre, Kampala; Baylor College of Medicine Children's Foundation,

570 Mulago Hospital, Kampala; MRC/UVRI Uganda Research Unit on AIDS, Entebbe) and
571 Zimbabwe (University of Zimbabwe, Harare)(33, 74). At baseline all participants were
572 receiving once-daily cotrimoxazole prophylaxis (200mg of sulfamethoxazole and 40mg of
573 trimethoprim, 400mg of sulfamethoxazole and 80mg of trimethoprim, or 800mg of
574 sulfamethoxazole and 160mg of trimethoprim for a body weight of 5-15, 15-30, or >30 kg,
575 respectively).

576

577 Participants were randomly assigned to stop (n=382) or continue (n=386) daily cotrimoxazole
578 prophylaxis as previously described(33, 74). Children were seen in clinic every 6 weeks to
579 record caregiver-reported symptoms of infection since the previous visit and measure height
580 and weight. CD4 count was measured and plasma stored (including for retrospective HIV
581 viral load testing) every 12 weeks post-randomization to a common trial end date (16th March
582 2012). Children were excluded from the original ARROW trial (for which ART was initiated
583 at enrolment) if they did not meet the 2006 WHO criteria for ART initiation(75), had acute
584 infections, had previously received ART or were perinatally exposed to ART (children <6
585 months old), were pregnant or breastfeeding, or were taking medications or had laboratory
586 abnormalities that contraindicated ART(74). Children were excluded from the subsequent
587 randomization to stop versus continue cotrimoxazole if they had a history of *Pneumocystis*
588 *jirovecii* pneumonia(33). 98% of children enrolled into ARROW during the last 6 months of
589 the recruitment period were also included in an immunology sub-study(5), and additional
590 assays were conducted for samples from these children as well as from a random 23% sample
591 of all remaining non-immunology sub-study children, as previously described(5).

592

594 Inclusion of children from the ARROW randomization trial and immunology sub-study in the
595 current study was determined by country of recruitment and sample availability, specified for
596 each sample-type below.

597

598 ***Circulating biomarker quantification***

599 CRP, TNF α , IL-6 and sCD14 were quantified via ELISA (Quantikine kits; R&D Systems
600 Inc.) in children with available plasma samples who were enrolled into the immunology sub-
601 study of ARROW in Uganda and Zimbabwe, and in all other children randomized to stop
602 versus continue cotrimoxazole in Zimbabwe. All children who had baseline measurements
603 (i.e. at randomization to stop versus continue cotrimoxazole) were included in statistical
604 comparisons between randomized groups at 12, 24, 48, 72 and 96 weeks post-randomization,
605 using the closest available measurement to each study time-point in equally spaced windows
606 (stop n=149 versus continue n=144).

607

608 For children known to have fasted for >6 hours prior to sample collection, total protein was
609 analyzed in one serum sample per child collected at week-48 post-randomization to stop
610 (n=151) or continue (n=159) cotrimoxazole (+/- 24 weeks; equivalent to 3 years after
611 enrolment to the ARROW trial and ART initiation). Albumin, and total protein were
612 quantified using a Beckman CX5 Delta Chemistry Analyzer (Beckman Coulter) as previously
613 described(76).

614

615 ***ARROW clinical symptoms***

617 Longitudinal caregiver-reported clinical symptoms since the last study visit (6-week recall of
618 incidents of cough, fever, abdominal pain/aching, nausea/vomiting, persistent, bloody or
619 moderate-to-severe diarrhea, difficult/fast breathing and weight loss), weight-for-age and
620 height-for-age Z scores were compared between the stop (baseline n=150) versus continue
621 (baseline n=145) groups for children who were also included in the plasma biomarker
622 quantification assays.

623

624 *Immunophenotyping of blood leukocytes*

625 Fresh whole blood was used to undertake T-cell immunophenotyping by flow cytometry in
626 the sub-set of ARROW children enrolled in the immunology sub-study in Uganda only and
627 for whom blood sample volumes were sufficient (stop n=48 versus continue n=47), as
628 previously described(5). Leukocytes were labelled with the following fluorophore-conjugated
629 antibodies: CD4-PerCP (BD Biosciences), CD31-PE (eBiosciences) and CD45RA-APC
630 (Caltag Medsystems) and Ki67-FITC (BD Biosciences; staining performed after membrane
631 permeabilization). Cell phenotyping was conducted on a BD FACSCalibur flow cytometer
632 and analyzed using CellQuest software (BD Biosciences; gating strategy is shown in **fig.**
633 **S1A**).

634

635 *Fecal inflammatory marker quantification*

636 Fecal samples were collected from children enrolled in the ARROW immunology sub-study
637 and randomized to stop (n=38) or continue (n=37) cotrimoxazole in Zimbabwe only at week-
638 84 and week-96 of follow-up. Myeloperoxidase, neopterin, α 1-antitrypsin, and REG1 β were

640 quantified in cryopreserved fecal samples using ELISA kits from Immun diagnostik AG,
641 Genway Biotech Inc, Immuchrom GmbH, and Techlab Inc, respectively.

642

643 ***Fecal DNA preparation and sequencing***

644 Total DNA was extracted from week-84 and week-96 150 mg fecal samples from 72 children
645 enrolled in the ARROW immunology sub-study in Zimbabwe (Stop n=36, Continue n=36)
646 using the MoBio DNA Extraction Kit with bead-beating modified for simultaneous RNA
647 isolation. Paired-end DNA libraries were prepared using Illumina® TruSeq® Nano DNA
648 Library Prep kits. As a quality control, the libraries were analyzed on a TapeStation 2200
649 before pooling. Whole metagenome sequencing was performed with 125-nucleotide paired-
650 end read lengths using the Illumina HiSeq 2500 platform at Canada's Michael Smith Genome
651 Sciences Centre, Vancouver, Canada. 23-24 libraries were pooled per sequencing lane.

652

653 Sequenced reads were trimmed of adapters and filtered to remove low-quality, short (<60
654 base-pairs), and duplicate reads, as well as those of human, other animal or plant origin using
655 KneadData with default settings. Species composition was determined by identifying clade-
656 specific markers from reads using MetaPhlan2 with default settings(77). Functional gene and
657 metabolic pathway composition was determined using HUMANN2 with default settings
658 against the UniRef90 database(78). Functionally annotated reads were further classified into
659 Pfam protein families(79) and level-4 enzyme commission (EC) categories using provided
660 scripts. Microbiome species, gene and pathway abundance were normalized by the total read
661 count in each stool sample (relative abundance). Median 10,507,352 versus 11,068,280

663 (p=0.23) reads were obtained at week-84, and 11,074,046 versus 10,875,436 (p=0.60) at
664 week-96 from continue and stop groups, respectively.

665

666 ***Microbiome analyses***

667 Alpha diversity was calculated at the species level using the inverse Shannon diversity index,
668 which provides a measure of the effective species number per fecal sample. Differences in
669 species relative abundance and diversity between randomized groups were evaluated at each
670 time-point by intention-to-treat analysis using linear regression models fitted against natural
671 log-transformed inverse Shannon diversity indices. Species diversity did not differ between
672 randomized groups at either visit (13.1 versus 14.3, p=0.27 and 13.5 versus 14.8, p=0.72).
673 Pielou's index of species evenness also showed no difference between randomized groups at
674 week-84 (mean 0.59 versus 0.60 in continue versus stop, p=0.605) or week-96 (mean 0.60
675 versus 0.61 in continue versus stop, p=0.883). Species-level beta diversity was evaluated
676 using the Bray–Curtis dissimilarity index, and visualized using NMDS.

677

678 Differences in species, Pfam, metabolic pathway and enzyme (microbiome characteristic)
679 relative abundance were evaluated at each time point by intention-to-treat analysis using
680 zero-inflated beta regression models fitted against relative abundances. Zero-inflated beta
681 regression is a two-part model with a logistic component to model the presence or absence of
682 each microbiome characteristic, and a beta component to model the non-zero relative
683 abundance, given that a microbiome characteristic is present. This model has been shown to
684 outperform other methods for identifying differentially abundant microbiome characteristics,

686 in terms of power and false discovery rate (FDR), due to its flexibility for handling non-
687 normal abundances with a large number of zeros(80, 81). Zero-inflated beta regression
688 models were fitted using generalized additive models for location, scale and shape with a log-
689 link(82), where the variance of the beta distribution was modeled as a function of sequencing
690 depth. Treatment effect was the ratio of relative microbiome characteristic abundance in the
691 continue group versus the stop group. A separate model was fit for each microbiome
692 characteristic. P-values were adjusted for multiple comparisons to maintain the FDR at the
693 desired significance level ($\alpha=0.05$)(83). Only differentially abundant microbiome
694 characteristics that were statistically significant at both week-84 and week-96 after FDR
695 adjustment were interpreted as causally related to long-term cotrimoxazole use. To determine
696 which species were responsible for the observed changes in functional composition,
697 differentially abundant protein families were further stratified by species, while differentially
698 abundant pathways were further stratified by species and pathway enzymes, and zero-inflated
699 beta-regression models were re-fitted with FDR correction.

700

701 We determined whether observed changes in microbiome composition were associated with
702 intestinal inflammation by fitting rank-based regression models against fecal
703 myeloperoxidase concentration adjusted for age, sex, and randomized group, with FDR
704 adjustment for multiple comparisons. In these analyses the week-84 and week-96 samples
705 were investigated independently.

706

707 To confirm species-level analyses in MetaPhlAn, PanPhlAn was used to pairwise map 140

709 ARROW datasets to 20 available Streptococcus pangenome databases in order to determine
710 the presence or absence of Streptococcus species at higher sensitivity(45). Default settings for
711 the programs panphlan_map.py and panphlan_profile.py were used(45).

712

713 All microbiome data analyses were conducted in *R* version 3.3.2. The package *VEGAN*(84),
714 was used to calculate the Shannon diversity and Bray-Curtis dissimilarity and NMDS.
715 *Gamlss* was used for zero-inflated beta regression(82). *Rfit* was used for rank-based
716 regression(85).

717

718 ***HIV-negative and HIV-positive UK adult participants***

719 HIV-negative adults were recruited via email circular to research staff at the Blizard Institute,
720 Queen Mary University of London, UK (n=8). HIV-positive adults on ART for >2 years
721 (n=6) or who were ART-naïve (n=10) were identified from outpatient records by clinicians
722 and nurses at the Grahame Hayton Unit of the Royal London Hospital, UK and invited to
723 participate during routine clinical appointments. Participants taking cotrimoxazole or other
724 antibiotics or with clinical signs of intercurrent infections were excluded from the study.
725 After written informed consent was provided, a 50 mL venous blood sample was collected
726 into sterile heparinized blood collection tubes (BD Biosciences) from each participant via
727 venipuncture. 10 mL of blood was used for immunophenotyping and whole blood culture.
728 PBMC and undiluted plasma were isolated from 40 mL of whole blood using Ficoll Plaque
729 Plus (GE Healthcare) density separation. Plasma samples were aliquoted and stored in
730 endotoxin-free cryovials (Greiner) at -80°C. Freshly isolated PBMC were washed twice in

732 sterile PBS/1% v/v Fetal Bovine Serum (FBS; Gibco) prior to staining and/or culture.

733

734 ***Plasma biomarker quantification***

735 Plasma CRP, sCD14, TNF α (Duoset kits from R&D Systems) and IL-6 (OptEIA kit from BD
 736 Biosciences) were quantified in all UK adult participants by ELISA.

737

738 ***Immunophenotyping of uncultured PBMC***

739 1×10^6 freshly isolated PBMC were incubated for 30 min with fluorophore-conjugated
 740 antibodies specific for T-cell and monocyte surface markers for 30 min (**table S2**), washed
 741 once in PBS/1% FBS and fixed for 30 min in Fixation buffer (eBiosciences). Labelling with
 742 fluorescence-minus-one (FMO) and isotype control antibodies for each surface marker and a
 743 membrane impermeable viability dye (Zombie aqua Fixable Viability dye; Biolegend) were
 744 conducted in parallel to determine hierarchical gating (gating strategy shown in **fig. S9B**).
 745 Immunophenotyping was conducted for all UK adult participants on a BD LSR II flow
 746 cytometer and analyzed using FlowJo LLC software version 10.

747

748 ***Antigens***

749 Lyophilized heat-killed *Salmonella typhimurium* (HKST), ultrapure lipopolysaccharide from
 750 *Escherichia coli* 0111:B4 strain (LPS), *Saccharomyces cerevisiae* cell wall (zymosan), and
 751 *Staphylococcus aureus* enterotoxin B (SEB; Sigma) were reconstituted according to the
 752 manufacturer's instructions.

754 **Drugs**

755 Trimethoprim and sulfamethoxazole were prepared in DMSO at a stock concentration of 100
 756 mg/mL (all from Sigma). Commercially available cotrimoxazole (100 mg/mL; Sigma) pre-
 757 formulated in DMSO was used for Caco-2 experiments. Drugs were titrated and assessed for
 758 antibiotic activity against bacterial isolates (**fig. S7A**), toxicity to cultured cells (**fig. S7B-D**;
 759 **Fig. 7B**), and optimal culture duration (**fig. S7E**) and timing of treatment relative to antigen
 760 stimulus (**fig. S7F**) prior to use in cell culture experiments. Controls for each cotrimoxazole
 761 treatment dose were prepared using DMSO without drug at the same total volume (i.e.
 762 volume of trimethoprim + volume of sulfamethoxazole). Final DMSO content in cultures
 763 were 0.05% v/v for CTX_[Low] and DMSO_[Low] controls and 0.2% v/v for CTX_[High] and
 764 DMSO_[High] controls.

765

766 **Whole blood culture**

767 Whole blood culture conditions for *in vitro* cotrimoxazole treatment were optimized using
 768 samples from HIV-negative adults (n=6; **fig. S7B, C, E and F**). Drug and antigen conditions
 769 for whole blood culture were batch-prepared in RPMI 1640 GlutaMAX™ (Gibco)
 770 supplemented with 1% v/v Penicillin-streptomycin (P-S; Gibco) and stored at -80°C. Single-
 771 use aliquots of drug and antigen conditions were thawed for each donor and combined with
 772 500 µL/well of 1:3 diluted blood (final concentrations in culture: blood at 1:6, HKST at 10⁸
 773 cells/mL, LPS at 5 EU/mL, and Zymosan at 5 µg/mL; low-dose cotrimoxazole (CTX_[Low]): 2
 774 µg/mL trimethoprim and 50 µg/mL sulfamethoxazole, high-dose cotrimoxazole (CTX_[High]): 8
 775 µg/mL trimethoprim and 200 µg/mL sulfamethoxazole). Whole blood cultures were

777 incubated for 24h at 37⁰C, 5% CO₂ after which cell-free supernatants were harvested and
 778 stored at -80⁰C. Cytokines in culture supernatants from all UK adults were quantified via
 779 sandwich ELISA (TNF α , R&D Duoset ELISA kits and IL-6, BD OptEIA ELISA Kits).

780

781 ***6h PBMC culture***

782 Drug and antigen conditions for PBMC culture were batch-prepared in RPMI 1640
 783 GlutaMAXTM/1% P-S/10% FBS (cRPMI) and stored at -80⁰C. Single-use aliquots of drug
 784 and antigen conditions were thawed for each donor and combined with 1x10⁶ PBMC in 50 μ L
 785 cRPMI with 100 μ l of pre-prepared drug condition (High dose CTX_[High] or volume-matched
 786 DMSO control), 50 μ l of pre-prepared antigen and 50 μ L cRPMI in sterile round-bottomed
 787 tubes (BD Biosciences). Final antigen concentrations in culture were: HKST at 10⁸ cells/ mL
 788 and SEB at 1 μ g/mL. PBMC cultures were incubated at 37⁰C, 5% CO₂. Brefeldin A (Sigma)
 789 was added to all cultures at a final concentration of 25 μ g/mL after 1h incubation. After a total
 790 of 6h culture, PBMC were washed in sterile PBS/1% FBS, labelled with fluorophore-
 791 conjugated antibodies specific for cell surface markers (**table S2**) for 30 min, washed in
 792 PBS/1% FBS and fixed overnight in fixation buffer (eBiosciences) at 4⁰C. Fixed cells were
 793 permeabilized in 1x Permeabilization buffer (eBiosciences) and labelled with fluorophore-
 794 conjugated antibodies specific for intracellular cytokines (**table S2**) for 40 min, washed once
 795 with Permeabilization buffer and once with PBS/1% FBS prior to analysis on a BD LSR II
 796 flow cytometer alongside FMO and isotype control-labelled samples (gating strategy shown
 797 in **fig. S9**). Analysis was conducted using FlowJo LLC software version 10.

798

800 ***Caco-2 transwell culture***

801 The human colonic epithelial cell-line Caco-2 derived from colorectal adenocarcinoma
802 (ATCC® HTB-37™) was maintained in DMEM (Lonza) supplemented with 1% v/v P-S,
803 1% v/v L-glutamine, 1% v/v Non-essential amino acids, and 10% v/v FBS (cDMEM; all
804 supplements from Gibco) in 75cm² culture flasks at 37⁰C, 5% CO₂. Cells were passaged on
805 reaching 80-90% confluency using Trypsin/EDTA (Gibco). Experiments were conducted
806 using Caco-2 between passage 35 and 40. Transwell cultures were conducted using 24-well
807 culture plates with Millicell Hanging Cell Culture Inserts (PET 0.4 μm; Merck-Millipore)
808 seeded apically with 1x10⁴ cells/well and cultured at 37⁰C, 5% CO₂. cDMEM was replaced
809 after the first 3 days of culture and every 2 days thereafter. TEER across the growing
810 monolayer was monitored daily using an STX04 test electrode with a Millicell® ERS-2-ohm
811 meter (Merck-Millipore). 1 mg/mL of cotrimoxazole, volume-matched DMSO or cDMEM
812 without drug was added apically to Caco-2 monolayers from the first day post-seed and
813 replenished at each media change during cell growth. Stimulation of the monolayers was
814 conducted when the plate mean TEER was >800Ω, which occurred between day 7-10 post-
815 seeding; individual wells with TEER <600Ω (i.e. sub-confluent) were excluded. Transwells
816 were stimulated apically with 1, 10 or 100 μg/mL recombinant human IL-1β (BioVision Inc)
817 or cDMEM without stimulus for 24h.

818

819 ***Caco-2 functional assays***

820 24h after stimuli were added, TEER was re-recorded and change in TEER calculated
821 (Δ TEER = 24h TEER - pre-treatment TEER), apical supernatants were harvested and stored

823 at -20⁰C and Caco-2 monolayers were washed once with sterile pre-warmed PBS and
824 transferred to new 24-well culture plates containing 1 mL/well sterile PBS pre-warmed to
825 37⁰C. 100 µg/mL Lucifer Yellow Biocytin dye (Molecular Probes) prepared in sterile pre-
826 warmed PBS was added to the apical side of each transwell and plates were incubated on a
827 plate shaker (100 rpm) at 37⁰C, 5% CO₂ for 1h. Fluorescence intensity (FI) was quantified in
828 apical and basal culture supernatants relative to an 11-point Lucifer Yellow standard curve
829 (100 – 0.1 µg/mL) using a BioTek plate reader (excitation/emission wavelength: 480/530nm);
830 %Lucifer Yellow apical-to-basal passage = $(FI_{\text{Basal}} - FI_{\text{PBS}}) / (FI_{100\mu\text{g/mL}} - FI_{\text{PBS}})$.

831

832 LDH activity and IL-8 were quantified in cryopreserved apical supernatants using LDH
833 Cytotoxicity Assay Kit (Pierce) and Human IL-8/CXCL8 DuoSet ELISA Kit (R&D Systems)
834 respectively. Apical supernatants from parallel Caco-2 transwell cultures treated with cell
835 lysis buffer (LDH_{Max}; Pierce) or an equivalent volume of sterile endotoxin-free ultrapure
836 water (LDH_{Spontaneous}) acted as controls for the LDH assay. LDH activity in drug-treated
837 cultures was calculated: %LDH = $(LDH_{\text{CTX}} - LDH_{\text{Spontaneous}}) / (LDH_{\text{Max}} - LDH_{\text{Spontaneous}}) \times 100$.

838

839 ***Statistical analysis***

840 For ARROW trial data, fold-change in geometric means between randomized groups were
841 compared for continuous variables (CRP, sCD14, IL-6 and TNFα in plasma; weight-for-age
842 and height-for-age Z scores; % CD4+ T-cells and their subsets) at each study time-point
843 using standard regression models and globally across all time-points using generalized
844 estimating equations (GEE; normal distribution for log transformed values), both with

846 adjustment for recruitment centre and baseline values, and assuming variation in treatment
847 effect by time-point. Proportions of children with HIV-1 viral load <80 copies/mL (viral
848 suppression) were compared between randomized groups at each time-point using Exact tests
849 and globally across all time-points using GEE (binomial distribution) with adjustment for
850 recruitment centre and assuming variation in treatment effect by time-point. Relative risk
851 projections for CRP and IL-6 differences between randomized groups were calculated from
852 the output of models based on pre-ART pre-cotrimoxazole biomarker levels in the ARROW
853 immunology sub-cohort, which we have previously reported(5). GEE and Exact tests were
854 conducted in STATA Software version 15.1 (StataCorp LLC). Concentrations of fecal
855 inflammatory markers at week-84 and week-96 and circulating proteins and lipids at week-48
856 post-randomization (Shapiro Wilk test for normality, $p < 0.05$) were compared between
857 randomized groups using the Mann-Whitney U test in Prism version 7.02 Software
858 (GraphPad).

859

860 For the *in vitro* cotrimoxazole treatment study, continuous variables (cytokine concentrations
861 and cell proportions; Shapiro-Wilk test for normality, $p < 0.05$) were compared between
862 clinical groups (HIV-negative, HIV-positive ART-treated and HIV-positive ART-naïve)
863 using unpaired Kruskal-Wallis tests. Comparisons between drug treatments were only
864 conducted where the response variable was significantly up-regulated in antigen-stimulated
865 cultures without drug treatment versus un-stimulated cultures without drug treatment, i.e.
866 cells were significantly activated to produce cytokines by the stimulus (paired Wilcoxon test,
867 $p < 0.05$). Comparisons between drug treatments were made within clinical groups using
868 Friedman tests with post-hoc pair-wise comparisons made using uncorrected Dunn's

870 tests; post-hoc tests were only conducted where the global test was statistically significant to
871 limit multiple comparisons.

872

873 Functional read-outs from Caco-2 cultures (TEER, Δ TEER, % LDH activity, % Lucifer
874 Yellow passage and IL-8 levels; Shapiro-Wilk test for normality, $p > 0.05$) were compared
875 between cotrimoxazole and DMSO-treated cultures using paired two-tailed t-tests. Analyses
876 included a minimum of 3 separate experiments (conducted using separate passages of Caco-
877 2) per culture condition. All analyses of *in vitro* cell culture models were conducted using
878 Prism version 7.02 software (GraphPad).

880 **REFERENCES**

- 881 1. UNAIDS, Fact sheet - Latest global and regional statistics on the status of the AIDS epidemic - July
882 2018. (2018).
- 883 2. J. A. Church, F. Fitzgerald, A. S. Walker, D. M. Gibb, A. J. Prendergast, The expanding role of co-
884 trimoxazole in developing countries. *The Lancet Infectious Diseases* **15**, 327-339 (2015).
- 885 3. A. S. Walker *et al.*, Daily co-trimoxazole prophylaxis in severely immunosuppressed HIV-infected
886 adults in Africa started on combination antiretroviral therapy: An observational analysis of the DART
887 cohort. *The Lancet* **375**, 1278-1286 (2010).
- 888 4. WHO, *Guidelines on post-exposure prophylaxis for HIV and the use of co-trimoxazole prophylaxis for*
889 *HIV-related infections among adults, adolescents and children: Recommendations for a public health*
890 *approach - December 2014 supplement to the 2013 consolidated ARV guidelines.* (WHO Press,
891 Geneva, Switzerland, 2014), pp. 49.
- 892 5. A. J. Prendergast *et al.*, Baseline inflammatory biomarkers identify subgroups of HIV-infected African
893 children with differing responses to antiretroviral therapy. *Journal of Infectious Diseases* **214**, 226-236
894 (2016).
- 895 6. L. H. Kuller, R. Tracy, W. Belloso, Inflammatory and coagulation biomarkers and mortality in patients
896 with HIV infection. *PLoS Medicine* **5**, (2008).
- 897 7. N. G. Sandler *et al.*, Plasma levels of soluble CD14 independently predict mortality in HIV infection.
898 *Journal of Infectious Diseases* **203**, 780-790 (2011).
- 899 8. P. W. Hunt, S. A. Lee, M. J. Siedner, Immunologic biomarkers, morbidity, and mortality in treated
900 HIV infection. *Journal of Infectious Diseases* **214**, S44-S50 (2016).
- 901 9. J. H. Campbell *et al.*, Minocycline Inhibition of Monocyte Activation Correlates with Neuronal
902 Protection in SIV NeuroAIDS. *PLoS ONE* **6**, e18688 (2011).
- 903 10. J. Vesterbacka *et al.*, Kinetics of microbial translocation markers in patients on Efavirenz or
904 Lopinavir/r based antiretroviral therapy. *PLoS ONE* **8**, e55038 (2013).
- 905 11. J. Vesterbacka, B. Barqasho, A. Haggblom, P. Nowak, Effects of co-trimoxazole on microbial
906 translocation in HIV-1-infected patients initiating antiretroviral therapy. *AIDS Research & Human*
907 *Retroviruses* **31**, 830-836 (2015).
- 908 12. J. M. Brenchley, T. W. Schacker, L. E. Ruff, CD4+ T cell depletion during all stages of HIV disease
909 occurs predominantly in the gastrointestinal tract. *Journal of Experimental Medicine* **200**, (2004).
- 910 13. M. Mavigner *et al.*, Altered CD4+ T cell homing to the gut impairs mucosal immune reconstitution in
911 treated HIV-infected individuals. *Journal of Clinical Investigation* **122**, 62-69 (2012).
- 912 14. K. Allers *et al.*, Macrophages accumulate in the gut mucosa of untreated HIV-infected patients.
913 *Journal of Infectious Diseases*, (2013).
- 914 15. M. Somsouk *et al.*, Gut epithelial barrier and systemic inflammation during chronic HIV infection.
915 *AIDS* **29**, 43-51 (2015).
- 916 16. J. M. Brenchley *et al.*, Microbial translocation is a cause of systemic immune activation in chronic HIV
917 infection. *Nat Med* **12**, 1365-1371 (2006).
- 918 17. A. P. Kourtis *et al.*, Role of intestinal mucosal integrity in HIV transmission to infants through breast-
919 feeding: the BAN study. *Journal of Infectious Diseases* **208**, 653-661 (2013).
- 920 18. C. Tincati, D. C. Douek, G. Marchetti, Gut barrier structure, mucosal immunity and intestinal
921 microbiota in the pathogenesis and treatment of HIV infection. *AIDS Research & Therapy* **13**, 19
922 (2016).
- 923 19. S. M. Dillon *et al.*, An altered intestinal mucosal microbiome in HIV-1 infection is associated with
924 mucosal and systemic immune activation and endotoxemia. *Mucosal immunology* **7**, 983-994 (2014).
- 925 20. G. Dubourg *et al.*, Gut microbiota associated with HIV infection is significantly enriched in bacteria
926 tolerant to oxygen. *BMJ Open Gastroenterology* **3**, e000080 (2016).
- 927 21. C. A. Lozupone *et al.*, Alterations in the gut microbiota associated with HIV-1 infection. *Cell Host &*
928 *Microbe* **14**, 10.1016/j.chom.2013.1008.1006 (2013).
- 929 22. D. M. Dinh, G. E. Volpe, C. Duffalo, Intestinal microbiota, microbial translocation, and systemic
930 inflammation in chronic HIV infection. *Journal of Infectious Diseases* **211**, (2015).
- 931 23. C. L. Monaco *et al.*, Altered virome and bacterial microbiome in Human Immunodeficiency Virus-
932 associated Acquired Immunodeficiency Syndrome. *Cell Host & Microbe* **19**, 311-322 (2016).
- 933 24. F. Dossou-Yovo *et al.*, Metronidazole or cotrimoxazole therapy is associated with a decrease in
934 intestinal bioavailability of common antiretroviral drugs. *PLoS ONE* **9**, e89943 (2014).

- 935 25. I. Pandrea *et al.*, Antibiotic and anti-inflammatory therapy transiently
936 reduces inflammation and hypercoagulation in acutely SIV-infected pigtailed macaques. *PLoS*
937 *Pathogens* **12**, e1005384 (2016).
- 938 26. M. W. Ghilchik, A. S. Morris, D. S. Reeves, Immunosuppressive powers of the antibacterial agent
939 trimethoprim. *Nature* **227**, 393-394 (1970).
- 940 27. G. Federico, M. Fantoni, F. Pallavicini, F. Ricci, A. Antinori, *In vivo* study in healthy volunteers on the
941 effect of tetracycline and cotrimoxazole on chemiluminescence and granulocyte adhesion. *Quaderni*
942 *Sclavo di diagnostica clinica e di laboratorio* **22**, 201-208 (1986).
- 943 28. R. Anderson, G. Grabow, R. Oosthuizen, A. Theron, A. J. Van Rensburg, Effects of sulfamethoxazole
944 and trimethoprim on human neutrophil and lymphocyte functions *in vitro*: *in vivo* effects of co-
945 trimoxazole. *Antimicrobial Agents & Chemotherapy* **17**, 322-326 (1980).
- 946 29. O. Pos, A. Steinhilber, P. L. Meenhorst, F. P. Kroon, R. Van Furth, Impaired phagocytosis of
947 *Staphylococcus aureus* by granulocytes and monocytes of AIDS patients. *Clinical & Experimental*
948 *Immunology* **88**, 23-28 (1992).
- 949 30. P. M. Gaylarde, I. Sarkany, Suppression of thymidine uptake of human lymphocytes by co-
950 trimoxazole. *British medical journal* **3**, 144-146 (1972).
- 951 31. N. M. Wolfish, N. Wassef, H. Gonzalez, C. Acharya, Immunologic parameters of children with urinary
952 tract infection: effects of trimethoprim-sulfamethoxazole. *Canadian Medical Association journal* **112**,
953 76-79 (1975).
- 954 32. V. Dubar *et al.*, The penetration of co-trimoxazole into alveolar macrophages and its effect on
955 inflammatory and immunoregulatory functions. *Journal of Antimicrobial Chemotherapy* **26**, 791-802
956 (1990).
- 957 33. M. Bwakura-Dangarembizi *et al.*, A randomized trial of prolonged co-trimoxazole in HIV-infected
958 children in Africa. *New England Journal of Medicine* **370**, 41-53 (2014).
- 959 34. E. K. Gough *et al.*, The impact of antibiotics on growth in children in low and middle income
960 countries: systematic review and meta-analysis of randomised controlled trials. *British medical journal*
961 **348**, g2267 (2014).
- 962 35. A. Prendergast, A. S. Walker, V. Mulenga, C. Chintu, D. M. Gibb, Improved growth and anemia in
963 HIV-infected African children taking cotrimoxazole prophylaxis. *Clinical infectious diseases : an*
964 *official publication of the Infectious Diseases Society of America* **52**, 953-956 (2011).
- 965 36. A. J. Prendergast *et al.*, Stunting is characterized by chronic inflammation in Zimbabwean infants.
966 *PLoS ONE* **9**, (2014).
- 967 37. S. Attia *et al.*, Mortality in children with complicated severe acute malnutrition is related to intestinal
968 and systemic inflammation: an observational cohort study. *The American Journal of Clinical Nutrition*,
969 (2016).
- 970 38. J. V. Giorgi, L. E. Hultin, J. A. McKeating, Shorter survival in advanced human immunodeficiency
971 virus type 1 infection is more closely associated with T lymphocyte activation than with plasma virus
972 burden or virus chemokine coreceptor usage. *Journal of Infectious Diseases* **179**, (1999).
- 973 39. Z. Liu *et al.*, Elevated CD38 antigen expression on CD8+ T cells is a stronger marker for the risk of
974 chronic HIV disease progression to AIDS and death in the Multicenter AIDS Cohort Study than CD4+
975 cell count, soluble immune activation markers, or combinations of HLA-DR and CD38 expression.
976 *Journal of Acquired Immune Deficiency Syndromes & Human Retrovirology* **16**, 83-92 (1997).
- 977 40. S. Tanaskovic, S. Fernandez, P. Price, S. Lee, M. A. French, CD31 (PECAM-1) is a marker of recent
978 thymic emigrants among CD4+ T-cells, but not CD8+ T-cells or $\gamma\delta$ T-cells, in HIV patients responding
979 to ART. *Immunology & Cell Biology* **88**, 321 (2010).
- 980 41. C. P. Neff *et al.*, Fecal microbiota composition drives immune activation in HIV-infected individuals.
981 *EBioMedicine* **30**, 192-202 (2018).
- 982 42. K. J. Marwa *et al.*, Resistance to cotrimoxazole and other antimicrobials among isolates from
983 HIV/AIDS and non-HIV/AIDS patients at Bugando Medical Centre, Mwanza, Tanzania. *AIDS*
984 *Research & Treatment* **2015**, 103874 (2015).
- 985 43. J. Mwansa, K. Mutela, I. Zulu, B. Amadi, P. Kelly, Antimicrobial sensitivity in Enterobacteria from
986 AIDS patients, Zambia. *Emerging Infectious Diseases* **8**, 92-93 (2002).
- 987 44. K. M. Powis *et al.*, Cotrimoxazole prophylaxis was associated with enteric commensal bacterial
988 resistance among HIV-exposed infants in a randomized controlled trial, Botswana. *Journal of the*
989 *International AIDS Society* **20**, e25021-n/a (2017).
- 990 45. M. Scholz *et al.*, Strain-level microbial epidemiology and population genomics from shotgun
991 metagenomics. *Nature methods* **13**, 435 (2016).

- 992 46. M. Choi *et al.*, Extracellular signal-regulated kinase inhibition by statins
993 inhibits neutrophil activation by ANCA. *Kidney international* **63**, 96-106 (2003).
994 47. S. Dunzendorfer *et al.*, Mevalonate-dependent inhibition of transendothelial migration and chemotaxis
995 of human peripheral blood neutrophils by pravastatin. *Circulation research* **81**, 963-969 (1997).
996 48. K. M. Harper, M. Mutasa, A. J. Prendergast, J. Humphrey, A. R. Manges, Environmental enteric
997 dysfunction pathways and child stunting: A systematic review. *PLoS neglected tropical diseases* **12**,
998 e0006205 (2018).
999 49. D. Lau *et al.*, Myeloperoxidase mediates neutrophil activation by association with CD11b/CD18
1000 integrins. *Proceedings of the National Academy of Sciences* **102**, 431-436 (2005).
1001 50. T. W. Chin, A. Vandembroucke, I. W. Fong, Pharmacokinetics of trimethoprim-sulfamethoxazole in
1002 critically ill and non-critically ill AIDS patients. *Antimicrobial Agents and Chemotherapy* **39**, 28-33
1003 (1995).
1004 51. N. T. Funderburg *et al.*, Rosuvastatin reduces vascular inflammation and T cell and monocyte
1005 activation in HIV-infected subjects on antiretroviral therapy. *Journal of Acquired Immune Deficiency
1006 Syndromes* **68**, 396-404 (2015).
1007 52. N. I. Paton, R. L. Goodall, D. T. Dunn, et al., Effects of hydroxychloroquine on immune activation and
1008 disease progression among HIV-infected patients not receiving antiretroviral therapy: A randomized
1009 controlled trial. *Journal of the American Medical Association* **308**, 353-361 (2012).
1010 53. J. P. Routy *et al.*, Assessment of chloroquine as a modulator of immune activation to improve CD4
1011 recovery in immune nonresponding HIV-infected patients receiving antiretroviral therapy. *HIV
1012 medicine* **16**, 48-56 (2015).
1013 54. R. D. Moore, J. G. Bartlett, J. E. Gallant, Association between use of HMG CoA reductase inhibitors
1014 and mortality in HIV-infected patients. *PLoS ONE* **6**, e21843 (2011).
1015 55. WHO, UNAIDS, Unicef, Global HIV/AIDS Epidemic update and health sector progress towards
1016 Universal Access. (2011).
1017 56. I. Sereti *et al.*, Persistent, albeit reduced, chronic inflammation in persons starting antiretroviral therapy
1018 in acute HIV infection. *Clinical infectious diseases : an official publication of the Infectious Diseases
1019 Society of America* **64**, 124-131 (2017).
1020 57. W. Jiang, M. M. Lederman, P. Hunt, Plasma levels of bacterial DNA correlate with immune activation
1021 and the magnitude of immune restoration in persons with antiretroviral-treated HIV infection. *Journal
1022 of Infectious Diseases* **199**, (2009).
1023 58. A. R. Tenorio *et al.*, Soluble markers of inflammation and coagulation but not T-Cell activation predict
1024 non-AIDS-defining morbid events during suppressive antiretroviral treatment. *Journal of Infectious
1025 Diseases* **210**, 1248-1259 (2014).
1026 59. M. D. Hazenberg *et al.*, Establishment of the CD4+ T-cell pool in healthy children and untreated
1027 children infected with HIV-1. *Blood* **104**, 3513-3519 (2004).
1028 60. C. D. Doern, C.-A. D. Burnham, It's not easy being green: the Viridans Group Streptococci, with a
1029 focus on pediatric clinical manifestations. *Journal of Clinical Microbiology* **48**, 3829-3835 (2010).
1030 61. B. Van den Bogert *et al.*, Comparative genomics analysis of Streptococcus isolates from the human
1031 small intestine reveals their adaptation to a highly dynamic ecosystem. *PLoS ONE* **8**, e83418 (2014).
1032 62. G. Li *et al.*, Diversity of duodenal and rectal microbiota in biopsy tissues and luminal contents in
1033 healthy volunteers. *Journal of Microbiology & Biotechnology* **25**, 1136-1145 (2015).
1034 63. P. Vonaesch *et al.*, Stunted childhood growth is associated with decompartmentalization of the
1035 gastrointestinal tract and overgrowth of oropharyngeal taxa. *Proceedings of the National Academy of
1036 Sciences* **115**, E8489-e8498 (2018).
1037 64. A. J. Prendergast *et al.*, Stunting is characterized by chronic inflammation in Zimbabwean infants.
1038 *PLoS ONE* **9**, e86928 (2014).
1039 65. B. van den Bogert, M. Meijerink, E. G. Zoetendal, J. M. Wells, M. Kleerebezem, Immunomodulatory
1040 properties of Streptococcus and Veillonella isolates from the human small intestine microbiota. *PLoS
1041 ONE* **9**, e114277 (2014).
1042 66. R. C. Allen, J. T. Stephens, Myeloperoxidase selectively binds and selectively kills microbes. *Infection
1043 & Immunity* **79**, 474-485 (2011).
1044 67. A. Abou-Eisha, A. Creus, R. Marcos, Genotoxic evaluation of the antimicrobial drug, trimethoprim, in
1045 cultured human lymphocytes. *Mutation research* **440**, 157-162 (1999).
1046 68. A. M. Ortiz *et al.*, Experimental microbial dysbiosis does not promote disease progression in SIV-
1047 infected macaques. *Nature Medicine* **24**, 1313-1316 (2018).
1048 69. S. Heuston, M. Begley, C. G. Gahan, C. Hill, Isoprenoid biosynthesis in bacterial pathogens.
1049 *Microbiology (Reading, England)* **158**, 1389-1401 (2012).

- 1050 70. M. A. Elmore, R. H. Daniels, M. E. Hill, M. J. Finnen, Inhibition of neutrophil priming by inhibitors of farnesyl transferase. *Biochemical Society transactions* **25**, 253s (1997).
- 1051
1052
1053 71. R. Terkeltaub, J. Solan, M. Barry, Jr., D. Santoro, G. M. Bokoch, Role of the mevalonate pathway of
1054 isoprenoid synthesis in IL-8 generation by activated monocytic cells. *Journal of leukocyte biology* **55**,
1055 749-755 (1994).
- 1056 72. E. Furrie *et al.*, Toll-like receptors-2, -3 and -4 expression patterns on human colon and their regulation
1057 by mucosal-associated bacteria. *Immunology* **115**, 565-574 (2005).
- 1058 73. J. D. Keenan *et al.*, Azithromycin to reduce childhood mortality in Sub-Saharan Africa. *New England*
1059 *Journal of Medicine* **378**, 1583-1592 (2018).
- 1060 74. A. Kekitiinwa *et al.*, Routine versus clinically driven laboratory monitoring and first-line antiretroviral
1061 therapy strategies in African children with HIV (ARROW): a 5-year open-label randomised factorial
1062 trial. *The Lancet* **381**, 1391-1403 (2013).
- 1063 75. *Antiretroviral therapy for HIV infection in infants and children: towards universal access:*
1064 *Recommendations for a public health approach* (2006).
- 1065 76. M. Bwakura-Dangarembizi *et al.*, Prevalence of lipodystrophy and metabolic abnormalities in HIV-
1066 infected African children after 3 years on first-line antiretroviral therapy. *Pediatric Infectious Diseases*
1067 *Journal* **34**, e23-31 (2015).
- 1068 77. D. T. Truong *et al.*, MetaPhlan2 for enhanced metagenomic taxonomic profiling. *Nature methods* **12**,
1069 902-903 (2015).
- 1070 78. S. Abubucker *et al.*, Metabolic reconstruction for metagenomic data and its application to the human
1071 microbiome. *PLoS Computational Biology* **8**, e1002358 (2012).
- 1072 79. R. D. Finn *et al.*, Pfam: the protein families database. *Nucleic acids research* **42**, D222-230 (2014).
- 1073 80. E. Z. Chen, H. Li, A two-part mixed-effects model for analyzing longitudinal microbiome
1074 compositional data. *Bioinformatics (Oxford, England)* **32**, 2611-2617 (2016).
- 1075 81. X. Peng, G. Li, Z. Liu, Zero-inflated Beta regression for differential abundance analysis with
1076 metagenomics data. *Journal of Computational Biology*, (2015).
- 1077 82. R. A. Rigby, D. M. Stasinopoulos, Generalized additive models for location, scale and shape. *Journal*
1078 *of the Royal Statistical Society: Series C (Applied Statistics)* **54**, 507-554 (2005).
- 1079 83. Y. Benjamini, Y. Hochberg, Controlling the False Discovery Rate: a practical and powerful approach
1080 to multiple testing. *Journal of the Royal Statistical Society. Series B (Methodological)* **57**, 289-300
1081 (1995).
- 1082 84. P. Dixon, M. W. Palmer, VEGAN, a package of R functions for community ecology. *Journal of*
1083 *Vegetation Science* **14**, 927-930 (2003).
- 1084 85. K. JD, J. McKean, Rfit: Rank-based estimation for linear models. *R Journal* **4**, 57-64 (2012).
- 1085
- 1086

1088 **ACKNOWLEDGEMENTS**

1089 We thank the participants, caregivers, and staff from all the centers participating in the
1090 ARROW trial and the *in vitro* cotrimoxazole treatment study. Antiretroviral drugs for the
1091 ARROW trial were donated and HIV viral load and genotyping assays were funded by ViiV
1092 Healthcare/GlaxoSmithKline. Cotrimoxazole for the ARROW trial was provided by national
1093 programs/Ministries for Health in Uganda and Zimbabwe. Margaret Govha and Sandra
1094 Rukobo undertook ELISA assays in Zimbabwe. Macklyn Kihembo and Lydia Nakiire
1095 undertook immunophenotyping at Uganda Virus Research Institute/Medical Research Centre,
1096 Entebbe and Joint Clinical Research Centre, Kampala, in Uganda, respectively. Hannah
1097 Poulosom provided supervision and assistance with ARROW assays. Anele Waters, Sarah
1098 Murphy and James Hand at the Grahame Hayton Unit, Royal London Hospital assisted with
1099 participant recruitment to the *in vitro* cotrimoxazole study. Aine McKnight hosted all
1100 containment level 3 laboratory work at QMUL.

1101

1102 **FUNDING**

1103 This study was funded by the Wellcome Trust (grants 093768/Z/10/Z and 108065/Z/15/Z to
1104 AJP), with operating funds sub-contracted to ARM. CDB is funded by a Sir Henry Dale
1105 Fellowship from the Wellcome Trust and the Royal Society, UK (206225/Z/17/Z). EKG was
1106 funded by a Canadian Institutes of Health Research Postdoctoral Fellowship. The ARROW
1107 trial was jointly funded by the UK Medical Research Council (MRC) grant numbers
1108 G0300400 (AJP, VM, MB-D, AK, NK, DMG, ASW) and G1001190 (AJP, VM, MB-D, AK,
1109 NK, DMG, ASW) and the UK Department for International Development (DFID) under the

1111 MRC/DFID Concordat agreement. It was also part of the EDCTP2 programme supported by
1112 the European Union. The MRC Clinical Trials Unit at UCL (AJS, MJS, DMG, ASW) is
1113 supported by funding from the MRC (MC_UU_12023/26). The funders and medication
1114 donors had no role in any aspect of the study design, data accrual, data analysis, writing of
1115 the manuscript, or the decision to submit the manuscript for publication.

1116

1117 **AUTHOR CONTRIBUTIONS**

1118 CDB and EKG: conceptualized and implemented experimental plans for *in vitro* studies and
1119 fecal microbiome respectively, analyzed the data, prepared the figures and tables and lead
1120 manuscript preparation. AS and CB conducted biomarker assays at the University of
1121 Zimbabwe. GP implemented biomarker assays at Joint Clinical Research Centre, Kampala,
1122 Uganda. LT screened and recruited HIV-positive donors in the UK with oversight from JRD
1123 and CDB. CDB recruited HIV-negative donors in the UK; LB and YK assisted CDB with
1124 implementation of ELISA and Caco-2 assays respectively. NC provided initial Caco-2 stocks
1125 and guidance on their maintenance. DMG and ASW conceptualised and managed the
1126 ARROW trial; NK, AJP, ASW, DMG, MJS and AJS conceptualised and managed the
1127 associated immunology and virology sub-studies within ARROW. MBD, VM, JL and AK,
1128 recruited and conducted clinical follow-up of patients in the ARROW trial. CB processed and
1129 stored all stool samples in the ARROW trial. KM managed viral load assays and stool ELISA
1130 in Zimbabwe. MG and HMG assisted EKG with implementation and analysis of microbiome
1131 assays. CP provided support for HIV assays in the UK. TJE and ARM conducted PanPhlAn
1132 analysis of microbiome data. ASW conducted statistical analysis of ARROW biomarkers and
1133 prepared the associated figures. ASW and AJS conducted predictive models of the effect of

1134

1135 CRP and IL-6 on relative risk of adverse outcomes. AJP and ARM conceptualized the
1136 project, developed the overall research plan and had primary responsibility for the final
1137 content of the manuscript. All authors read and contributed to the manuscript, provided
1138 critical revisions, and approved its submission. None of the authors reported a conflict of
1139 interest related to the study. CDB and EKG contributed equally to this work. ARM and AJP
1140 also contributed equally to this work.

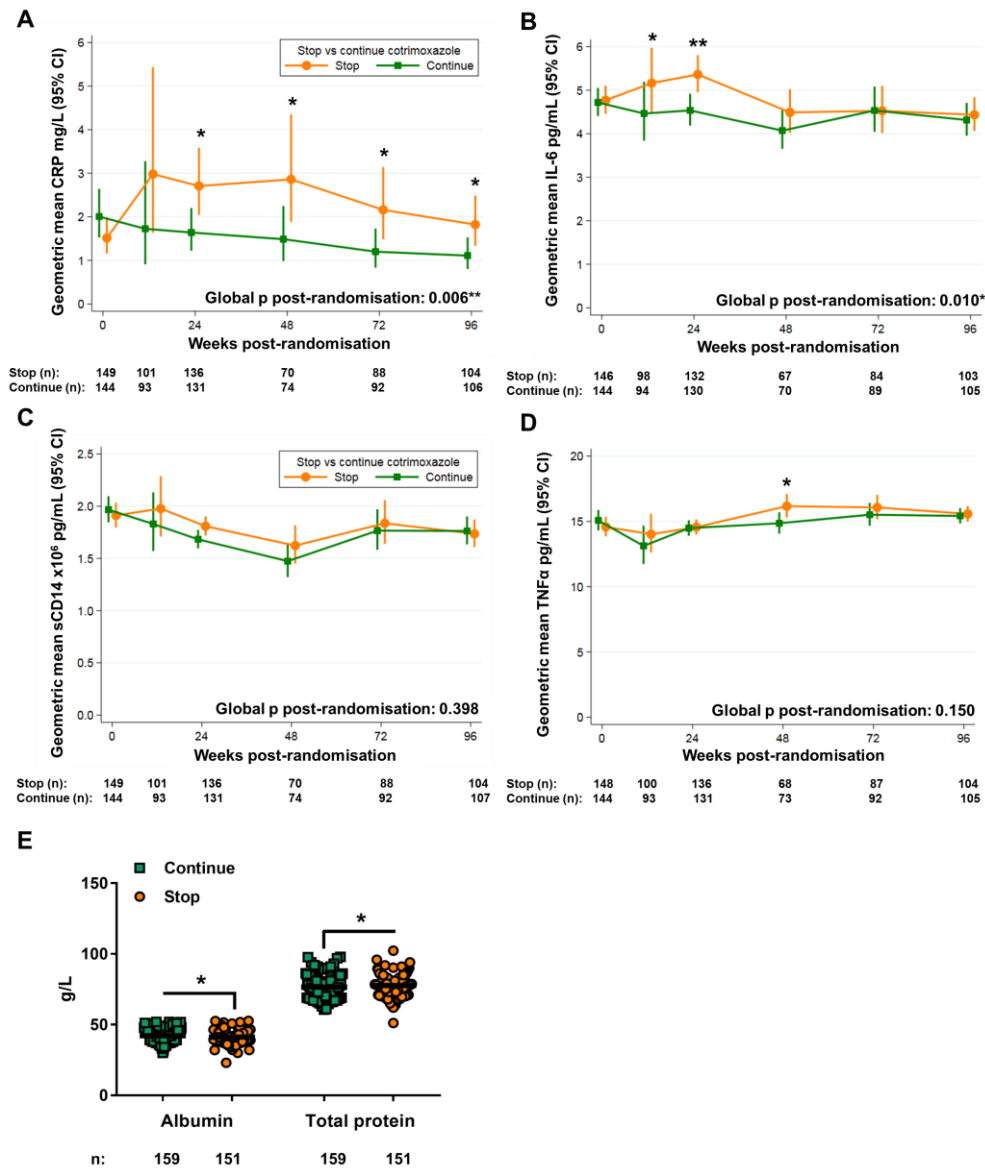
1141

1142 **COMPETING INTERESTS**

1143 The authors declare no competing interests.

1144

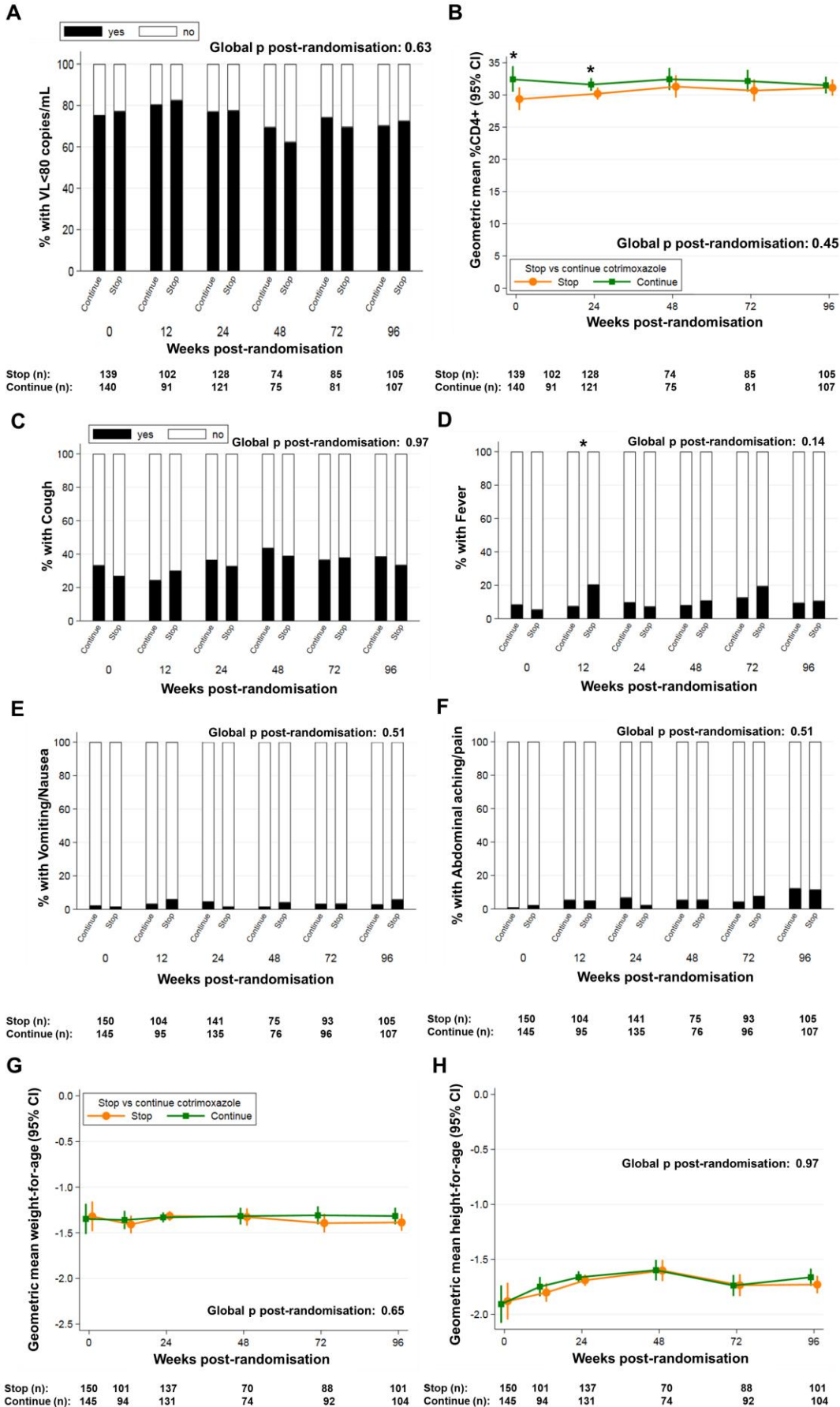
1146 FIGURES



1147

1148 **Figure 1. Systemic inflammation is lower among HIV-positive children randomized to**
 1149 **continue daily oral cotrimoxazole prophylaxis.** Biomarkers of systemic inflammation in
 1150 longitudinal plasma samples from Zimbabwean and Ugandan children who had been
 1151 receiving ART for ≥ 96 weeks with daily cotrimoxazole who were then randomized to stop
 1152 (orange circles) or continue (green squares) cotrimoxazole. Geometric mean levels of (A)

1154 CRP, **(B)** IL-6, **(C)** TNF α , and **(D)** sCD14 in plasma. Randomized groups were compared
1155 across all time-points using generalized estimating equations and at individual time-points
1156 using standard regression models (binomial distribution for viral load suppression, otherwise
1157 normal distribution for log-transformed values), all adjusted for centre and baseline
1158 biomarker levels (global p; **A-D**); *p<0.05, **p<0.01 ***p<0.001. **(E)** Serum levels of
1159 protein at week-48 post-randomization; horizontal bars indicate means. Comparisons between
1160 groups were made by Mann-Whitney U test; *p<0.05, **p<0.01 ***p<0.001.



1163 **Figure 2. Cotrimoxazole effects on systemic inflammation are not solely due to**
1164 **differences in HIV disease progression, symptomatic infections or nutritional status. (A)**
1165 Percentage of children with HIV suppression (viral load <80 copies/mL), **(B)** geometric mean
1166 percentage CD4+ T-cells, proportions of children with caregiver-reported **(C)** cough, **(D)**
1167 fever, **(E)** vomiting/nausea and **(F)** abdominal pain, geometric mean **(G)** weight-for-age and
1168 **(H)** height-for-age Z scores were quantified longitudinally in children randomized to
1169 continue versus stop cotrimoxazole prophylaxis. The number of samples per randomized
1170 group is shown under each graph. Longitudinal data were compared between randomized
1171 groups by generalized estimating equations across all time-points (global p) and at individual
1172 time-points using standard regression models (binomial distribution for viral load
1173 suppression, otherwise normal distribution for log transformed values) adjusted for
1174 recruitment centre; *p<0.05, **p<0.01 ***p<0.001.

1175

1176

1177

1178

1179

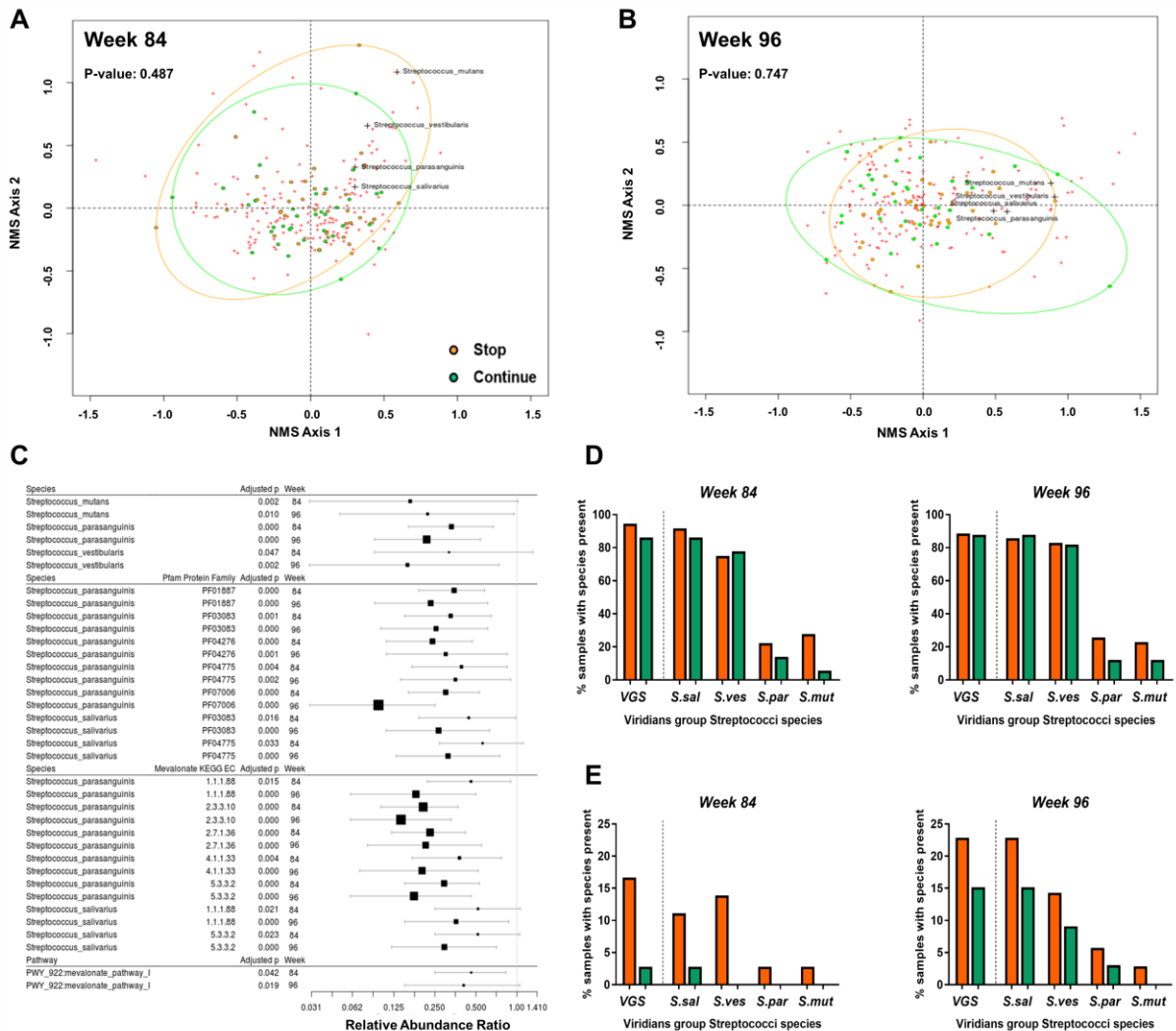
1180

1181

1182

1183

1184



1185

1186 **Figure 3. Continuation of cotrimoxazole specifically suppresses the abundance and**

1187 **function of viridians group Streptococci in randomized fecal samples from HIV-positive**

1188 **children. Non-metric multidimensional scaling (NMS) plots of the Bray–Curtis dissimilarity**

1189 **index of species-level fecal microbiomes from 72 HIV-positive Zimbabwean children**

1190 **randomized to stop (orange) versus continue (green) cotrimoxazole prophylaxis in the**

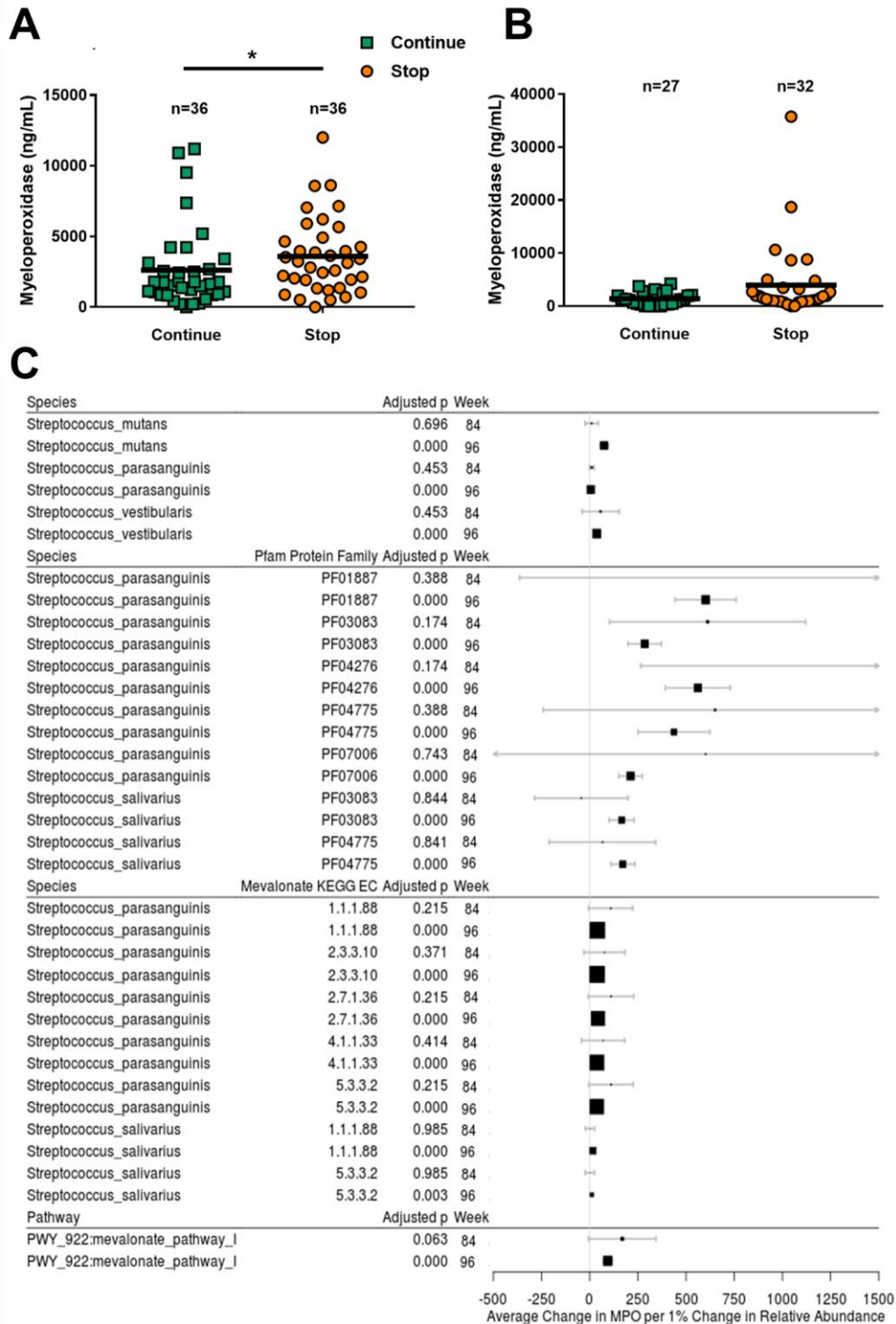
1191 **ARROW trial at (A) week-84 and (B) week-96 post-randomization. Each dot represents the**

1192 **global fecal bacterial species community composition of each child and the distance between**

1193 **them indicates their relative similarity/dissimilarity. Red crosses indicate distribution of**

1194 **individual bacterial species within the cohort irrespective of randomized group; VGS species**

1196 that consistently differed according to cotrimoxazole treatment are labelled. Results of
 1197 permutation tests for global differences between randomized cotrimoxazole treatment groups
 1198 are indicated. (C) Effect size plots showing relative abundance ratios (\pm 95% confidence
 1199 interval) for all *Streptococcus* spp. and the protein families (Pfam), metabolic pathways and
 1200 mevalonate pathway-associated genes with identity to *Streptococcus* spp. that significantly
 1201 differed in abundance between children who continued versus those who stopped
 1202 cotrimoxazole at both week-84 and week-96 post-randomization in zero-inflated beta
 1203 regression analysis after FDR adjustment for multiple hypothesis testing. The identities of
 1204 bacterial species for each Pfam and mevalonate enzyme were established using HUMANn2
 1205 with default settings against the UniRef90 database. Relative abundance ratio less than 1.0
 1206 indicates a decrease in relative abundance in children randomized to continue versus stop
 1207 cotrimoxazole. The size of the squares is inversely proportional to the magnitude of the FDR-
 1208 adjusted p values. The vertical grey line indicates the null value. Effect size plots for full lists
 1209 of differentially abundant species and Pfam, are available in **fig. S2** and **S3**. Percentage of
 1210 samples that were positive for any of the four VGS or individual species according to (D)
 1211 MetaPhlAn and (E) PanPhlAn analysis at week-84 (Continue n=36 and Stop n=36) and week-
 1212 96 (Continue n=33 and Stop n=35).



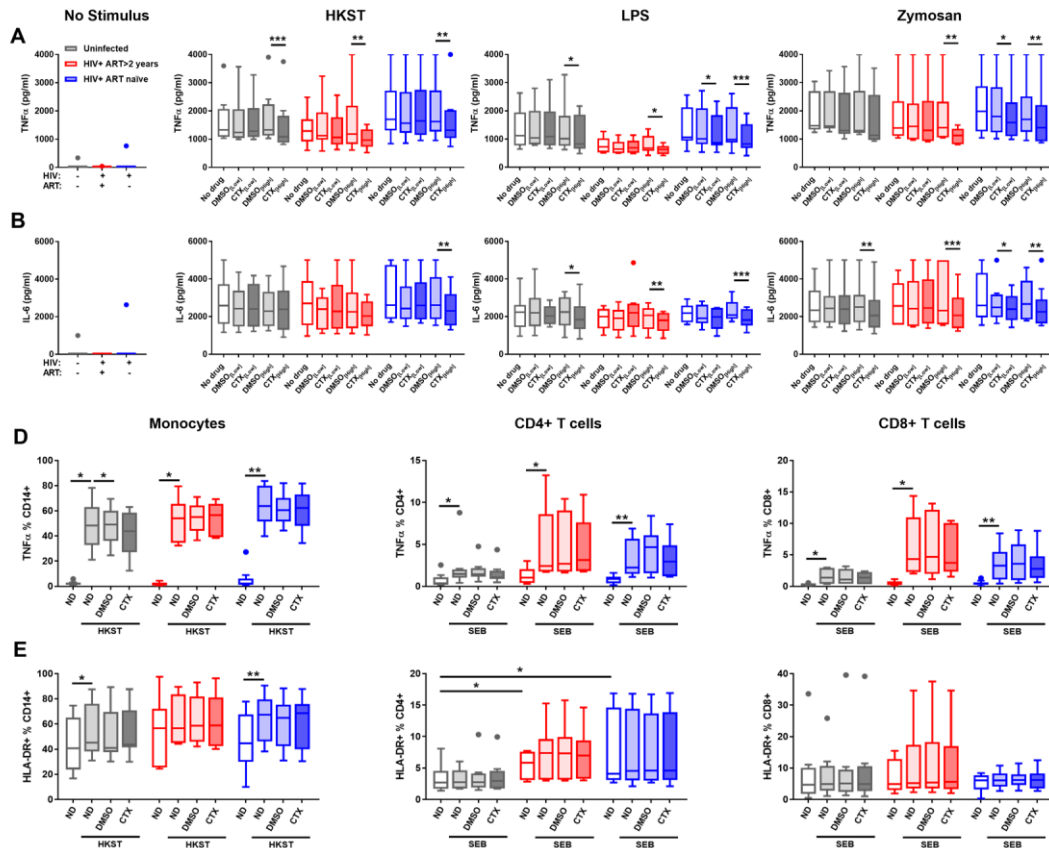
1213

1214 **Figure 4. Intestinal inflammation is positively associated with fecal viridians group**

1215 **Streptococci that are suppressed by continuation of cotrimoxazole prophylaxis among**

1216 **HIV-positive children. Myeloperoxidase levels assayed at (A) week-84 and (B) week-96 in**

1218 fecal samples from HIV-positive Zimbabwean children randomized to stop versus continue
 1219 cotrimoxazole prophylaxis. Randomized groups were compared by Mann-Whitney U test;
 1220 * $p < 0.05$, horizontal lines indicate the median value. (C) Effect size plots showing the average
 1221 change in myeloperoxidase per 1% change in relative abundance (\pm 95% confidence interval)
 1222 for all *Streptococcus* spp., and their protein families (Pfam), metabolic pathways and
 1223 mevalonate pathway-associated genes that significantly differed in abundance between
 1224 children who continued versus those who stopped cotrimoxazole at both week-84 and week-
 1225 96 post-randomization in zero-inflated beta regression analysis after FDR adjustment for
 1226 multiple hypothesis testing (**Fig. 3C**). Identities of bacterial species for each Pfam and
 1227 mevalonate enzyme were established using HUMANN2 with default settings against the
 1228 UniRef90 database. The size of the squares is inversely proportional to the magnitude of the
 1229 FDR-adjusted p values. The vertical grey line indicates the null value. Effect size plots for full
 1230 lists of differentially abundant species and Pfam are available in **fig. S5** and **S6**.
 1231



1232

1233

1234

Figure 5. Cotrimoxazole inhibits *in vitro* pro-inflammatory cytokine responses to

1235

bacterial and fungal antigens. Tukey boxplots of (A) TNF α and (B) IL-6 levels in

1236

supernatants from whole blood cultures without antigen (No stimulus; far left), with 10⁸

1237

cells/mL heat-killed *Salmonella typhimurium* (HKST; centre left), 5 EU/mL

1238

lipopolysaccharide (LPS; centre right); or 5 μ g/mL zymosan (far right). Cultures were treated

1239

with low-dose (CTX_[Low]: 2 μ g/mL trimethoprim and 50 μ g/mL sulfamethoxazole), high-dose

1240

cotrimoxazole (CTX_[High]: 8 μ g/mL trimethoprim and 200 μ g/mL sulfamethoxazole) or

1241

volume-matched diluent controls (DMSO_[Low] or DMSO_[High]). Proportions of monocytes

1242

(left), CD4+ (centre) and CD8+ T-cells producing (C) TNF α and expressing (D) HLA-DR

1243

after 6h PBMC culture. Blood samples from HIV-negative adults are in grey (n=8); HIV-

1244

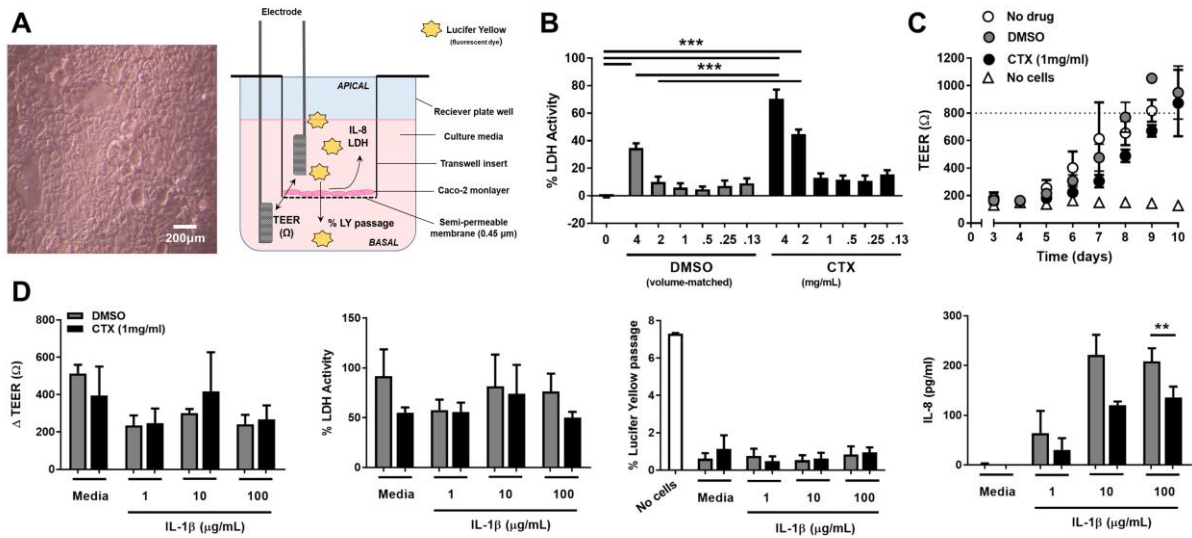
positive ART-treated adults are in red (n=6); and HIV-positive ART-naïve adults are in blue

1245

1246](n=10). Cytokine levels in cotrimoxazole-treated cultures are indicated by darker shading.

1247 Drug treatments were compared within groups by Friedman tests with post-hoc Dunn's tests;

1248 *p<0.05, **p<0.01, ***p<0.001.



1249

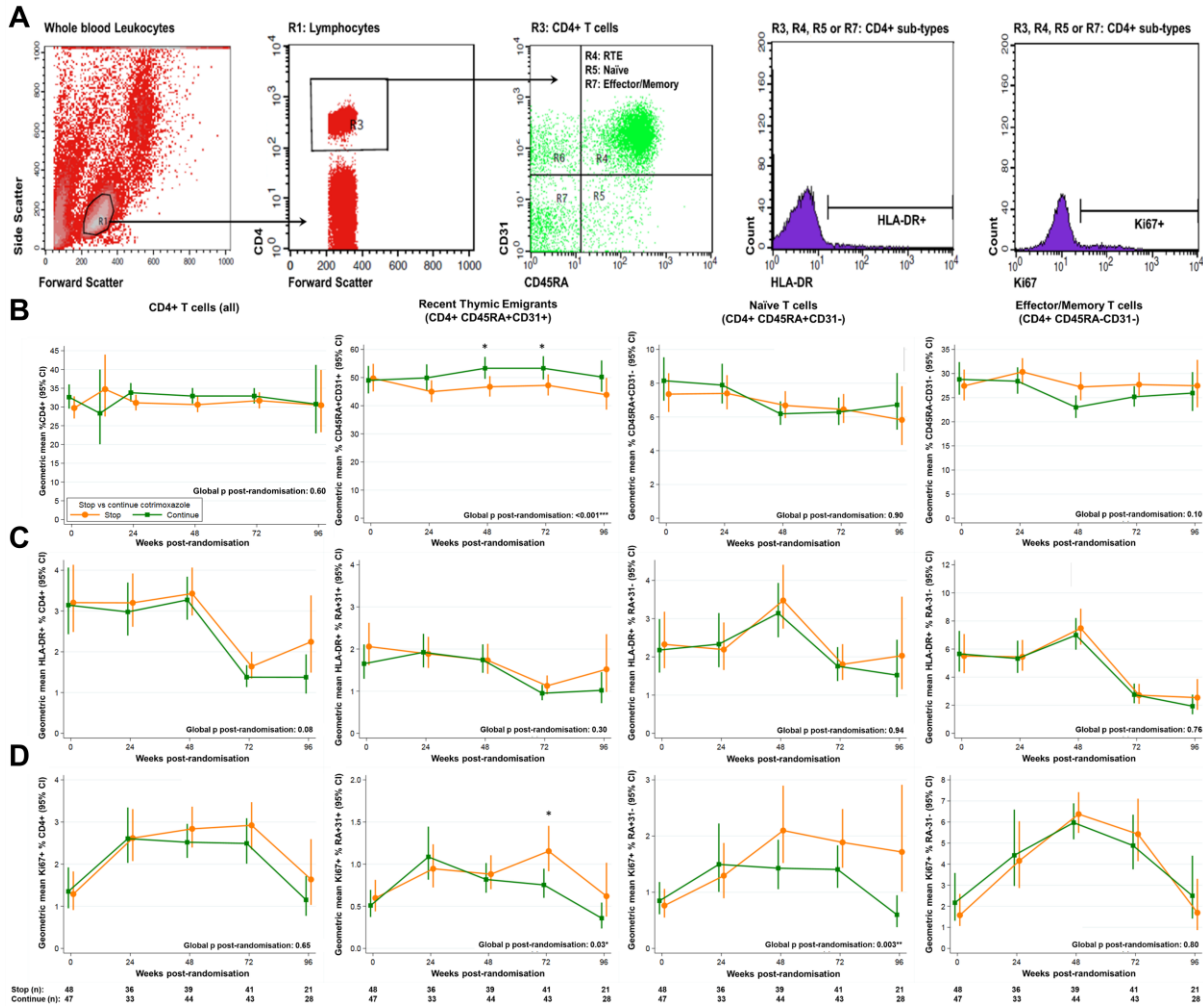
1250 **Figure 6. Long-term cotrimoxazole treatment reduces *in vitro* IL-8 production by gut**
 1251 **epithelial cell monolayers under inflammatory conditions. (A)** Light microscopy of
 1252 confluent Caco-2 monolayer (200 μm scale bar; left) and a diagram of the transwell culture
 1253 model (right). **(B)** Percentage lactose dehydrogenase activity relative to lysed cells (% LDH)
 1254 of Caco-2 monolayers cultured for 24h with titrated concentrations of cotrimoxazole (CTX;
 1255 black bars) or DMSO control (grey bars); % LDH was compared to untreated controls and
 1256 between volume-matched pairs of cotrimoxazole and DMSO by Tukey's test adjusted for
 1257 multiple comparisons; ***p<0.001. **(C)** Daily trans-epithelial resistance (TEER)
 1258 measurements of transwell Caco-2 cultures with no drug (white circles), 1 mg/mL
 1259 cotrimoxazole (black circles) or volume-matched DMSO control (grey circles) present
 1260 throughout growth relative to transwells without Caco-2 (no cells; white triangles); mean ±
 1261 SEM, n=3 separate experiments. Dotted line indicates the mean 800Ω TEER/plate threshold
 1262 for stimulating cultures. **(D)** Caco-2 transwell cultures that had been treated with 1 mg/mL
 1263 CTX or DMSO since seeding were incubated for 24h with media alone (no stimulus) or IL-
 1264 1β at 1 μg/mL, 10 μg/mL or 100 μg/mL for 24h; mean ± SEM, n=3 separate experiments. For
 1265 each experiment, graphs indicate the change in TEER from pre- to 24h post-treatment (Δ

1266

1267 TEER; far left), % LDH (centre left), % apical-to-basal passage of Lucifer Yellow dye
1268 relative to transwells without Caco-2 cells (centre right), and IL-8 concentration in apical
1269 supernatants (far right). Comparisons between cotrimoxazole- and DMSO-treated cultures
1270 were made by 2-tailed t-tests; * $p < 0.05$, ** $p < 0.01$

1271

1273 SUPPLEMENTARY MATERIALS



1274

1275

1276 **figure S1. Cotrimoxazole alters circulating CD4+ T-cell phenotype in HIV infection. (A)**

1277 Representative gating of flow cytometry data from uncultured blood leukocytes from HIV-

1278 positive ART-treated children randomized to stop (orange circles) versus continue (green

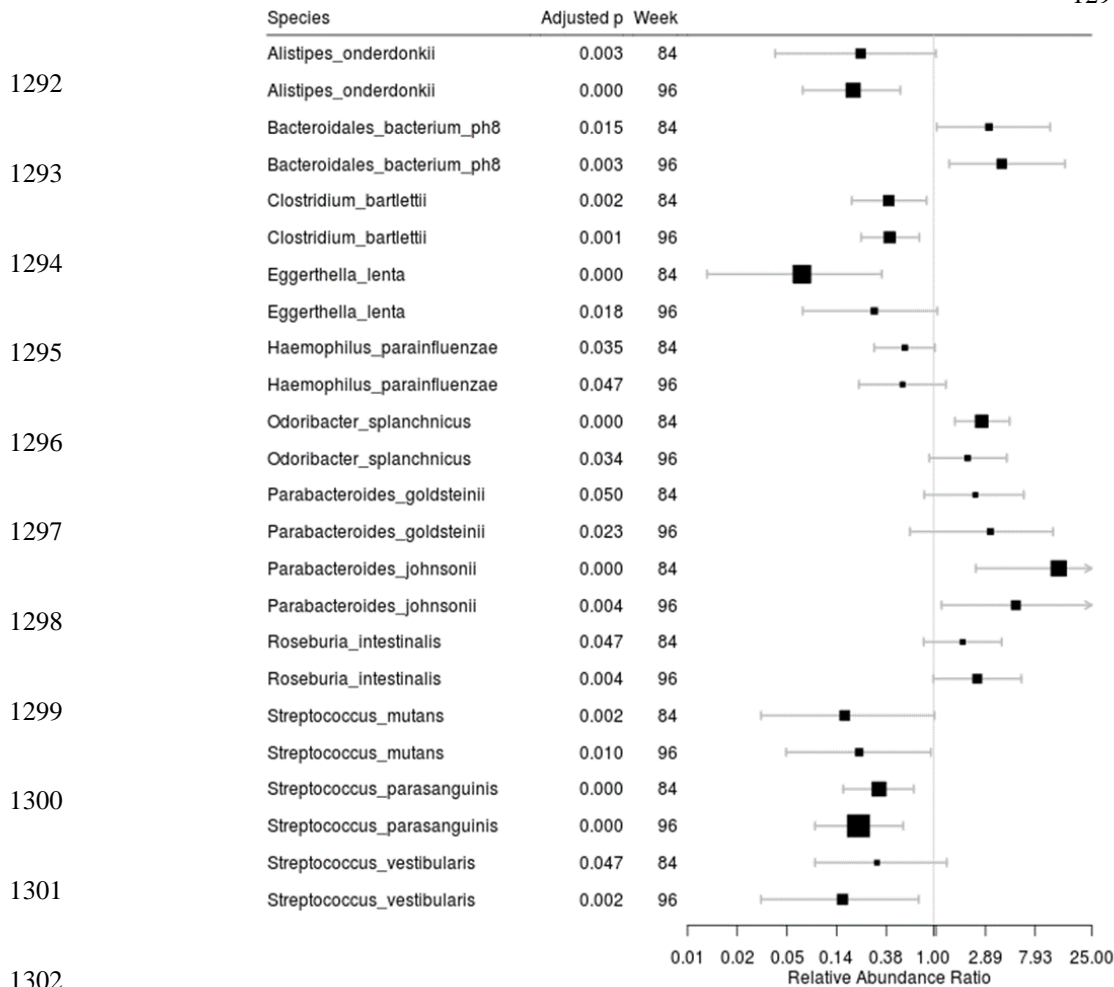
1279 squares) cotrimoxazole prophylaxis. Lymphocytes (R1) were gated on CD4 expression (R3)

1280 and sub-divided according to CD31 and CD45RA expression into: recent thymic emigrant-

1281 like (RTE; CD45RA+ CD31+; R4), naïve (CD45RA+ CD31-; R5) or effector-memory

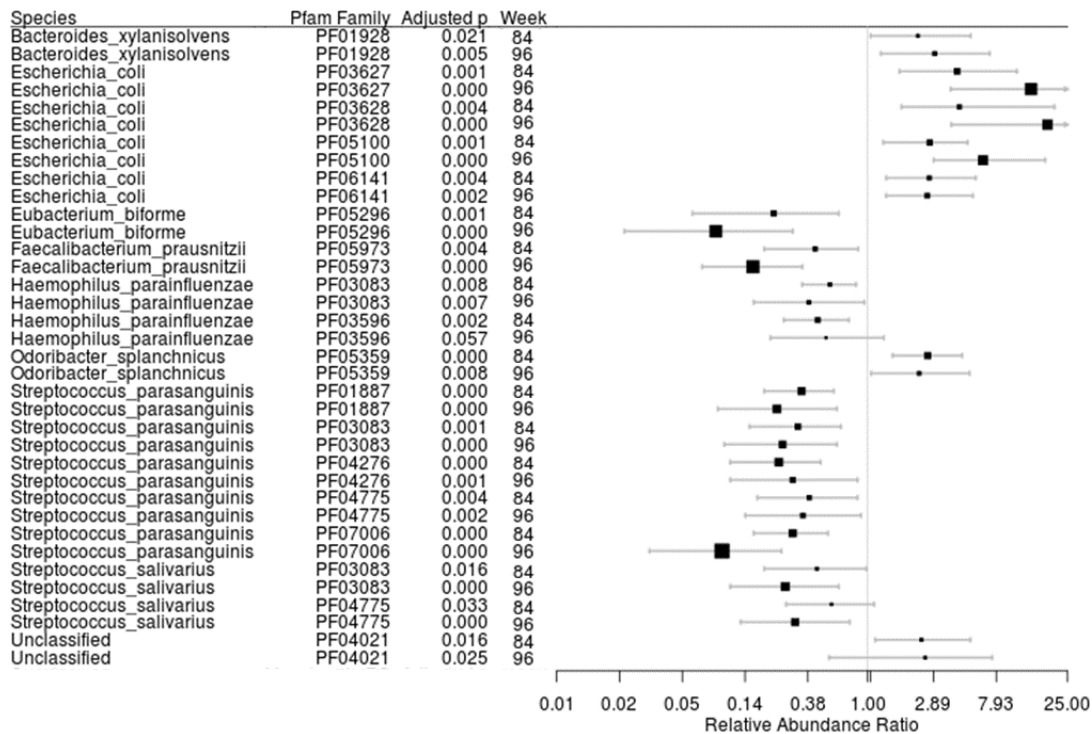
1282

1283 (CD45RA-CD31-; R7) CD4+ T-cells. Graphs show the proportions of CD4+ T-cell subsets
1284 (B) and the proportion of each subset expressing the surface activation marker HLA-DR (C)
1285 or the intracellular proliferation marker Ki67 (D). Numbers of participants at each time-point
1286 are indicated below the graphs. Statistical comparisons between randomized groups were
1287 made using generalized estimating equations across all time-points (global p) and at
1288 individual time-points using standard regression models (normal distribution for log
1289 transformed values), all adjusted for centre and baseline percentages; *p<0.05, **p<0.01
1290 ***p<0.001



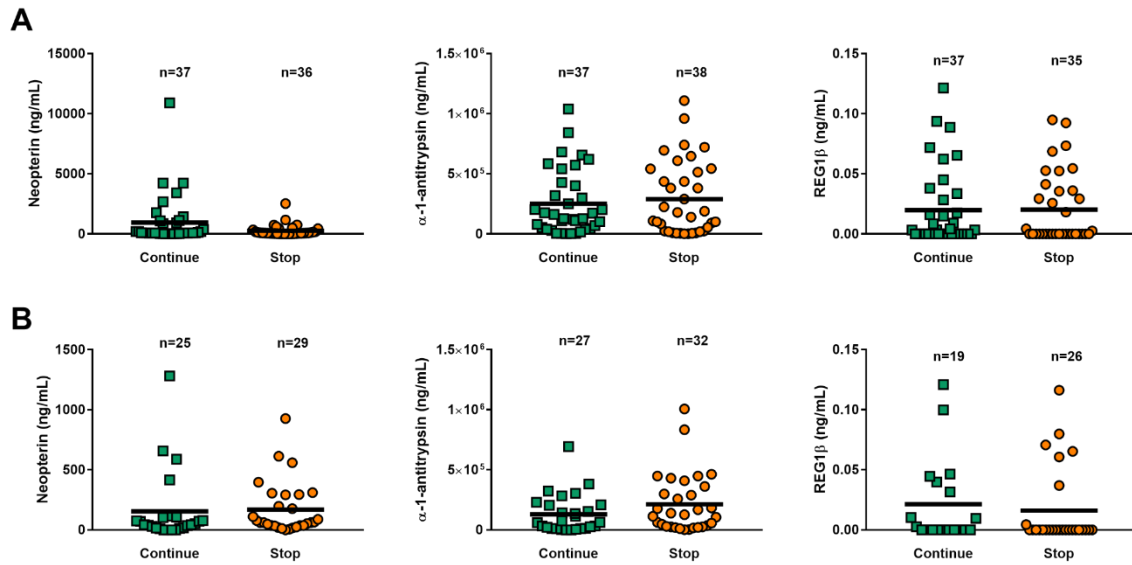
1303 **figure S2. Fecal bacterial species that differ between HIV-positive ART-treated**
 1304 **Zimbabwean children randomized to continue versus stop cotrimoxazole prophylaxis.**
 1305 Effect size plots (relative abundance ratios \pm 95% confidence interval) of bacterial species
 1306 that had a consistent statistically significant difference in relative abundance at both week-84
 1307 and week-96 post-randomization to continue (n=36) versus stop (n=36) cotrimoxazole after
 1308 FDR adjustment for multiple hypothesis testing (adjusted p<0.05). Relative abundance ratio
 1309 less than 1.0 indicates a decrease in relative abundance in children randomized to continue
 1310 versus stop cotrimoxazole. The size of the squares is inversely proportional to the magnitude
 1311 of the FDR-adjusted p values. Vertical grey line indicates the null value. Comparison
 1312 between randomized groups was made by zero-inflated beta regression.

1313



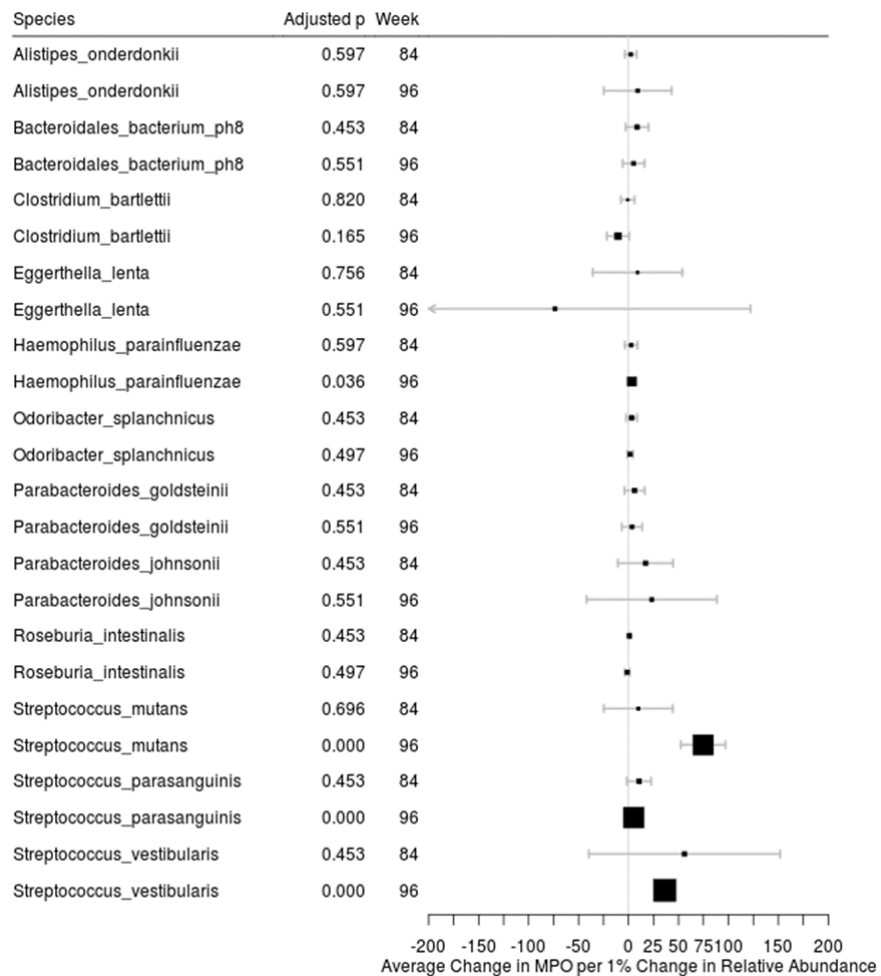
1314

1315 **figure S3. Protein families that differ in fecal samples between HIV-positive ART-**
 1316 **treated Zimbabwean children randomized to continue versus stop cotrimoxazole**
 1317 **prophylaxis.** Effect size plots (relative abundance ratios \pm 95% confidence interval) of
 1318 protein families (Pfam) that had a consistent statistically significant difference in relative
 1319 abundance at both week-84 and week-96 post-randomization to continue (n=36) versus stop
 1320 (n=36) cotrimoxazole after FDR adjustment for multiple hypothesis testing (adjusted
 1321 $p < 0.05$). Identities of bacterial species for each Pfam were established using HUMANn2 with
 1322 default settings against the UniRef90 database. Relative abundance ratio less than 1.0
 1323 indicates a decrease in relative abundance in children randomized to continue versus stop
 1324 cotrimoxazole. The size of the squares is inversely proportional to the magnitude of the FDR-
 1325 adjusted p values. Vertical grey line indicates the null value. Comparison between
 1326 randomized groups was made by zero-inflated beta regression.



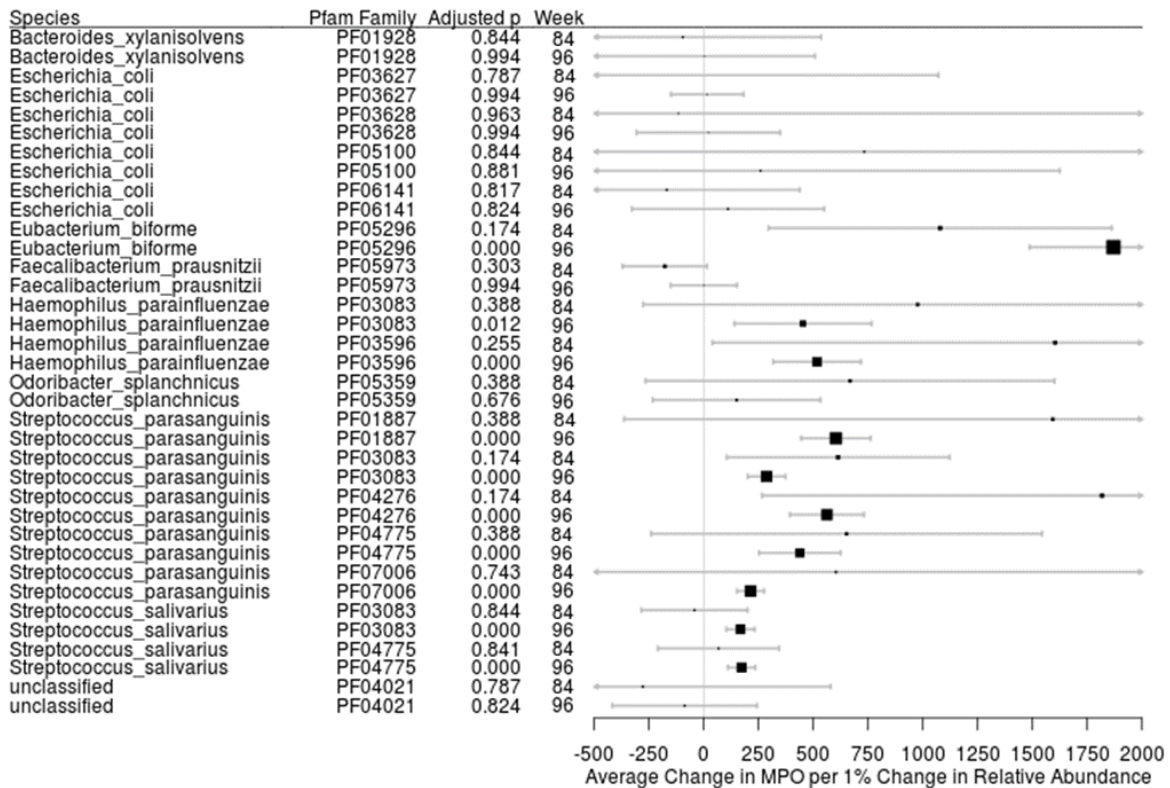
1327

1328 **figure S4. Fecal biomarkers of enteropathy that were unaffected by continuing versus**
 1329 **stopping cotrimoxazole prophylaxis.** Concentrations of the enteropathy biomarkers
 1330 neopterin, α -1-antitrypsin and regenerating family member 1 beta (REG1 β) in fecal samples
 1331 collected from HIV-positive ART-treated Zimbabwean children randomized to stop (orange
 1332 circles) or continue (green squares) cotrimoxazole prophylaxis at (A) week-84 and (B) week-
 1333 96 post-randomization within the ARROW trial. Comparisons were made between
 1334 randomized groups by Mann-Whitney U test; $p > 0.05$.



1335

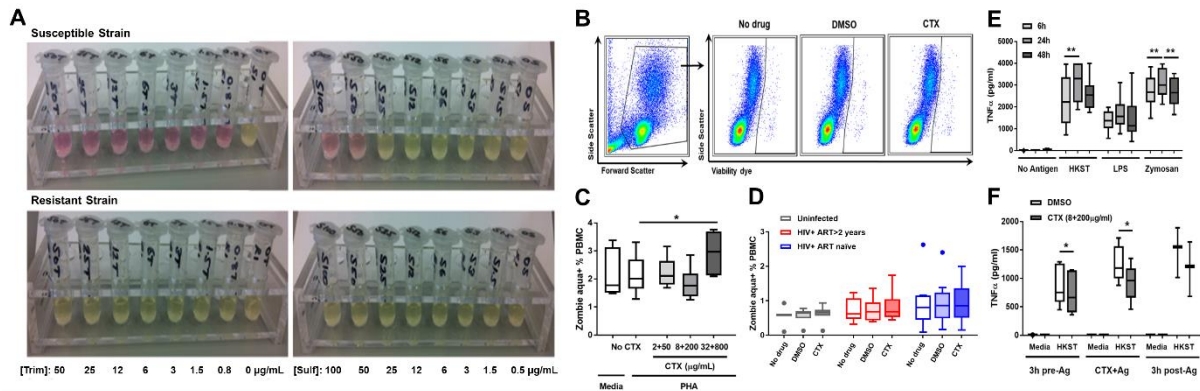
1336 **figure S5. Associations between all fecal bacterial species that differed between HIV-**
 1337 **positive children randomized to continue versus stop cotrimoxazole prophylaxis and fecal**
 1338 **levels of myeloperoxidase.** Effect size plots showing the average change in fecal
 1339 myeloperoxidase per 1% change in relative abundance (\pm 95% confidence interval) for all
 1340 bacterial species that significantly differed in abundance between fecal samples from children
 1341 randomized to continue versus stop cotrimoxazole at both week-84 and week-96 post-
 1342 randomization in zero-inflated beta regression analysis after FDR adjustment for multiple
 1343 hypothesis testing. The size of the squares is inversely proportional to the magnitude of the
 1344 FDR-adjusted p values. The vertical grey line indicates the null value. **Fig. 4C** presents a
 1345 condensed version of this analysis for *Streptococcal* spp.



1347

1348 **figure S6. Associations between all fecal Pfam that differed between HIV-positive**
1349 **children randomized to continue versus stop cotrimoxazole prophylaxis and fecal levels**
1350 **of myeloperoxidase.** Effect size plots showing the average change in fecal myeloperoxidase
1351 per 1% change in relative abundance (\pm 95% confidence interval) for all Pfam that
1352 significantly differed in abundance between fecal samples children randomized to continue
1353 versus stop cotrimoxazole at both week-84 and week-96 post-randomization in zero-inflated
1354 beta regression analysis after FDR adjustment for multiple hypothesis testing. Identities of
1355 bacterial species for each Pfam were established using HUMANN2 with default settings
1356 against the UniRef90 database. The size of the squares is inversely proportional to the
1357 magnitude of the FDR-adjusted p values. The vertical grey line indicates the null value. **Fig.**
1358 **4C** presents a condensed version of this analysis for Pfam with identify to *Streptococcal* spp.

1359



1361

1362

figure S7. Optimization of *in vitro* blood leukocyte activation and cotrimoxazole

1363

treatment conditions. (A) Photographs of 24h cultures of cotrimoxazole-susceptible (isolate

1364

ID: 15A076507S; top) and cotrimoxazole-resistant (isolate ID: 15A076598R; bottom)

1365

bacterial isolates from human urinary tract infections treated with titrated concentrations of

1366

trimethoprim (Trim, left) and sulfamethoxazole (Sulf, right) prepared in DMSO diluent;

1367

representative of 2 experimental repeats. Pink transparent media indicates an absence of

1368

bacterial growth, confirming that laboratory preparations of cotrimoxazole have antibiotic

1369

activity at minimum concentrations of 0.8 $\mu\text{g}/\text{mL}$ trimethoprim and 50 $\mu\text{g}/\text{mL}$

1370

sulfamethoxazole. A yellow opaque appearance indicates bacterial growth, which, as

1371

expected, is not inhibited by co-culture of trimethoprim or sulfamethoxazole with resistant

1372

bacteria. **(B)** Flow cytometry gating strategy showing Zombie aqua cell viability staining

1373

(Biologend; positive staining identifies dead cells) of unstimulated PBMC cultured for 6h

1374

without drug treatment, with cotrimoxazole (CTX: 8 $\mu\text{g}/\text{mL}$ trimethoprim and 200 $\mu\text{g}/\text{mL}$

1375

sulfamethoxazole) or volume-matched DMSO control; representative of 24 samples. **(C)**

1376

Tukey boxplots showing median proportions of dead (Zombie aqua+) PBMC after 24h

1377

culture without antigen or with 1 $\mu\text{g}/\text{mL}$ of mitogen (PHA) with titrated concentrations of

1378

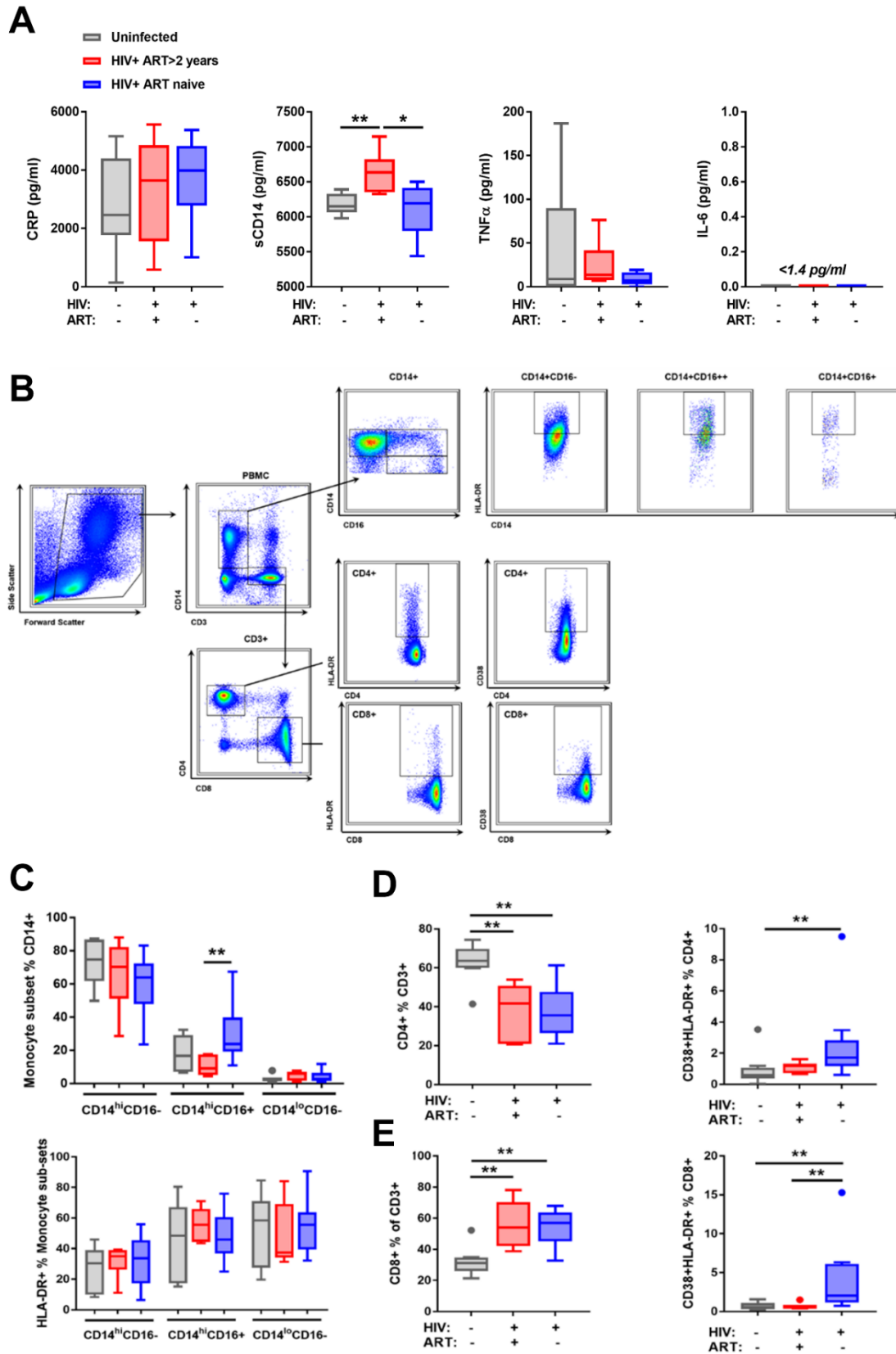
cotrimoxazole. Cell death significantly increased at concentrations of 32 $\mu\text{g}/\text{mL}$ trimethoprim

1379

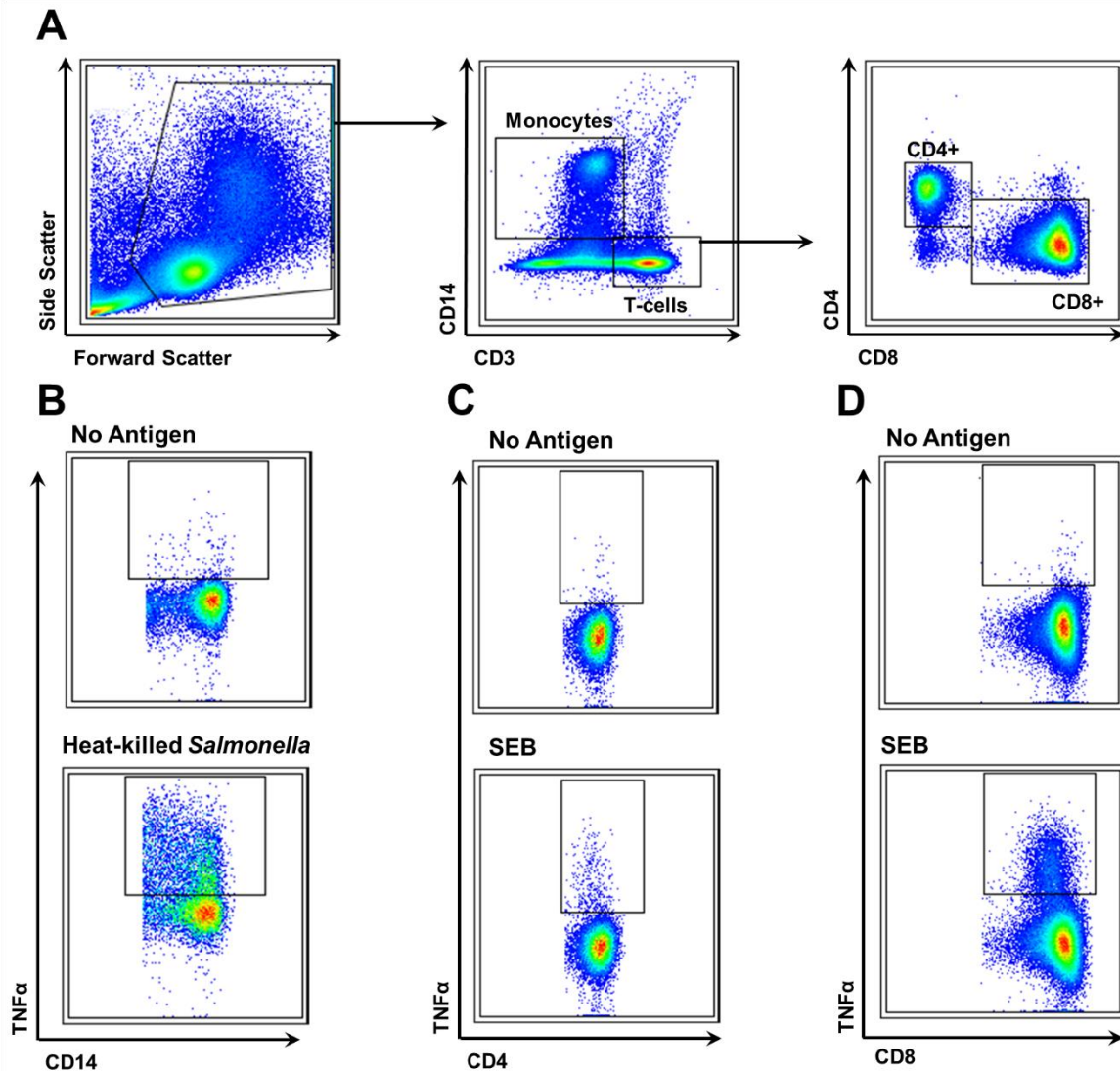
1380

1381 and 800µg/mL sulfamethoxazole, therefore subsequent *in vitro* doses were maintained below
1382 this threshold. Freidman's test with post-hoc uncorrected Dunn's; n=6, *p<0.05. (D) Tukey
1383 boxplots showing median proportions of dead (Zombie aqua+) cells in unstimulated 6h
1384 PBMC from HIV-negative (n=8, grey), HIV-positive ART-treated (n=8, red) and HIV-
1385 positive ART-naïve (n=10, blue) adults cultured for 6h without drug (ND) or with CTX at 8
1386 µg/mL trimethoprim and 200 µg/mL sulfamethoxazole or volume-matched DMSO. None of
1387 the drug treatments affected cell viability relative to untreated cultures. (E) Tukey boxplots
1388 showing median TNFα concentrations in whole blood culture supernatants after 6, 24 or 48h
1389 culture with bacterial and fungal TLR ligands; Kruskal-Wallis with post-hoc uncorrected
1390 Dunn's test; n=6, **p<0.01. (F) Tukey boxplots showing median TNFα concentrations in
1391 whole blood culture supernatants after 24h culture with HKST and addition of CTX (8+200
1392 µg/mL) for 3h before (3h pre-Ag), at the same time as (CTX+Ag) or 3h after (3h-post Ag)
1393 addition of HKST; Mann-Whitney U test; n=6, *p<0.05. 24h culture with TLR ligands and
1394 simultaneous cotrimoxazole treatment were chosen for subsequent experiments.

1395



1399 **figure S8. HIV-positive adults have greater systemic inflammation, monocyte and T-cell**
1400 **activation than HIV-negative adults.** Background inflammation and circulating immune
1401 cell activation was assessed in blood samples from HIV-negative (grey; n=8), HIV-positive
1402 ART-treated (red; n=6) and HIV-positive ART-naïve adults (blue; n=10) recruited in the UK
1403 (A) Levels of systemic inflammatory mediators in plasma samples. Levels of IL-6 were
1404 below the ELISA limit of detection in all three groups (<1.4 pg/mL). Statistical comparisons
1405 between groups were made using Kruskal-Wallis test with post-hoc pair-wise Dunn's test;
1406 *p<0.05, **p<0.01. (B) Representative flow cytometry gating strategy for monocyte and T-
1407 cell phenotyping in freshly isolated PBMC; representative of 24 samples. (C) Monocyte
1408 activation phenotype: proportions of monocyte sub-types segregated according to CD14 and
1409 CD16 expression (classical CD14^{hi}CD16⁻; intermediate CD14^{hi}CD16⁺; and non-classical
1410 CD14^{lo}CD16⁺; above), and HLA-DR expression by monocyte sub-types (below). Proportions
1411 of (D) CD4⁺ and (E) CD8⁺ T-cells within the CD3⁺ T-cell pool (left) and proportions of T-
1412 cells co-expressing HLA-DR and CD38 markers associated with activation. Statistical
1413 comparisons between groups were made using Kruskal-Wallis test with post-hoc pair-wise
1414 Dunn's test; *p<0.05, **p<0.01.



1416

1417 **figure S9. Flow cytometry gating strategy for analysis of monocyte and T-cell**

1418 **intracellular cytokine responses.** (A) Flow cytometry gating strategy for identification of

1419 monocytes (CD14+) and T-cells (CD3+, sub-divided by CD4 and CD8 expression) in PBMC

1420 cultured for 6h. (B) Flow cytometry gating of TNF α -expressing monocytes after 6h culture

1421 without antigen or with 10^8 cells/mL of heat-killed *Salmonella typhimurium*. Flow cytometry

1422 gating of TNF α -expressing (C) CD4+ and (D) CD8+ T-cells after 6h culture without antigen

1423 or with 1 μ g/mL Staphylococcal enterotoxin B (SEB). Flow cytometry plots are

1424 representative of 24 PBMC cultures conducted without drug treatment.

table S1. Characteristics of HIV-negative and HIV-positive UK adult volunteers

	HIV-	HIV+ ART >2 years	HIV+ ART naïve ¹
n	8	6	10
Gender (M, F)	7, 1	6, 0	8, 2
Age (range)	38 (27-59)	59 (41 -81)	40 (27 - 61)
HIV viral load (copies/mL)	-	<40	17,225 (<40 - 78,318)
CD4 count (cells/mm³)	-	545 (211-826)	585 (278 - 997)
Years on ART (range)	-	10 (4-17)	-

Mean values are shown.

¹One participant in group 2 was an ‘elite controller’ (viral load <40 copies/mL, CD4 count: 723 cells/mm³); minimum viral load of non-elite controller participants in the HIV+ ART naïve group was 615 copies/mL.

table S2. Details of fluorophore-conjugated antibody combinations used for flow cytometry analysis of PBMC from HIV-negative and HIV-positive adults.

Target	Clone	Isotype	Fluorophore	Manufacturer	Catalogue#
Uncultured PBMC Phenotyping Panel					
CD16	3G8	IgG1	Pacific Blue	BioLegend	302032
CD38	HB7	IgG1	BV 510	BioLegend	356612
CD14	M5E2	IgG2a, κ	BV 605	BioLegend	301834
CD3	UCHT1	IgG1, κ	FITC	BioLegend	300406
CD4	OKT4	IgG2b, κ	PE	eBiosciences	12-0048-42
CD8a	SK1	IgG1, κ	PE-Cy7	eBiosciences	25-0087-42
HLA-DR	L243	IgG2a, κ	APC-Cy7	BioLegend	307618
Cultured PBMC Intracellular Cytokine Panel					
CD3	UCHT1	IgG1, κ	Pacific Blue	BioLegend	300431
CD4	OKT4	IgG2b, κ	BV 510	BioLegend	317444
CD14	M5E2	IgG2a, κ	BV 605	BioLegend	301834
TNF α	MAb11	IgG1, κ	PE	eBiosciences	12-7349-81
CD8a	SK1	IgG1, κ	PE-Cy7	eBiosciences	25-0087-42
HLA-DR	L243	IgG2a, κ	APC-Cy7	BioLegend	307618

BV - Brilliant Violet; EF - eBiosciences Fluor; AF - Alexa Fluor